

การถ่ายโอนประจุของออกซิเจนกับไฮโดรเจนไอออนที่อุณหภูมิสูง

นายเสรี พงศ์พันธุ์ภาณี



สถาบันวิทยบริการ
จุฬาลงกรณ์มหาวิทยาลัย

วิทยานิพนธ์นี้เป็นส่วนหนึ่งของการศึกษาตามหลักสูตรปริญญาวิทยาศาสตรมหาบัณฑิต

สาขาวิชาฟิสิกส์ ภาควิชาฟิสิกส์

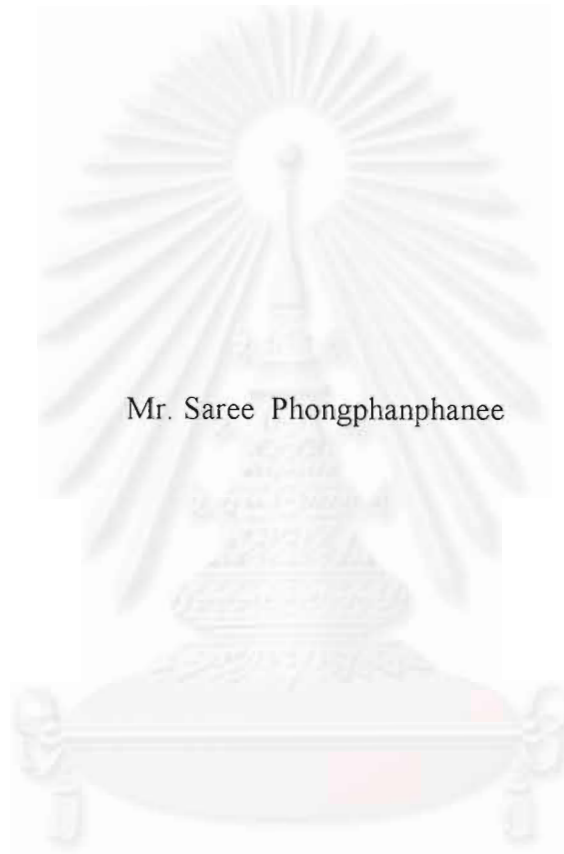
คณะวิทยาศาสตร์ จุฬาลงกรณ์มหาวิทยาลัย

ปีการศึกษา 2542

ISBN 974-334-042-4

ลิขสิทธิ์ของจุฬาลงกรณ์มหาวิทยาลัย

CHARGE TRANSFER OF O WITH H^+ AT HIGH TEMPERATURES



Mr. Saree Phongphananee

สถาบันวิทยบริการ
จุฬาลงกรณ์มหาวิทยาลัย

A Thesis Submitted in Partial Fulfillment of the Requirements

for the Degree of Master of Science in Physics

Department of Physics

Faculty of Sciences

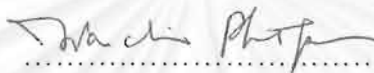
Chulalongkorn University

Academic Year 1999

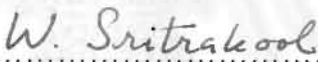
ISBN 974-334-042-4

Thesis Title Charge Transfer of O with H⁺ at High Temperatures
By Mr. Saree Phongphananee
Department Physics
Thesis Advisor Associate Professor David Ruffolo, Ph.D.
Thesis Co-advisor Associate Professor Vudhichai Parasuk, Ph.D.

Accepted by the Faculty of Science, Chulalongkorn University in Partial
Fulfillment of the Requirements for the Master's Degree



..... Dean of Faculty of Science
(Associate Professor Wanchai Phothiphichitr, Ph.D.)

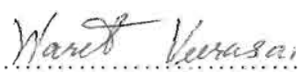
Thesis Committee


..... Chairman
(Associate Professor Wichit Sritrakool, Ph.D.)


..... Thesis Advisor
(Associate Professor David Ruffolo, Ph.D.)


..... Thesis Co-advisor
(Associate Professor Vudhichai Parasuk, Ph.D.)


..... Member
(Assistant Professor Kajornyod Yoodee, Ph.D.)


..... Member
(Waret Veerasai, Dr. rer. nat.)

เสรี พงศ์พันธุ์ภาณี: การถ่ายโอนประจุของออกซิเจนกับไฮโดรเจนไอออนที่อุณหภูมิสูง. (CHARGE TRANSFER OF O WITH H⁺ AT HIGH TEMPERATURES) อ. ที่ปรึกษา : รศ.ดร. เดวิด รุฟไฟโ-
โล, อ. ที่ปรึกษาร่วม : รศ. ดร. วุฒิชัย พาราสุข , 65 หน้า. ISBN 974-334-042-4.

เราได้ศึกษาการถ่ายโอนประจุระหว่างอะตอมออกซิเจน และไฮโดรเจนไอออน ในช่วงความเร็ว 400-800 กิโลเมตรต่อวินาที (0.18-0.36 หน่วยอะตอม) ซึ่งยังไม่เคยมีผลการคำนวณหรือการทดลองในตลอดช่วงพลังงานนี้ เราได้ใช้วิธีการ ควอนตัมคัปปลิงและวิธีการกึ่งแบบฉบับ ในการคำนวณครั้งนี้ค่าศักย์แอเดียแบติกและนอนแอเดียแบติกคัปปลิง ได้มาจากงานตีพิมพ์ที่ผ่านมา ค่าของภาคตัดขวางที่ได้จากการคำนวณของทั้งสองวิธีการได้ค่าอันดับเดียวกับผลของการคำนวณและการทดลองที่ผ่านมา ส่วนผลของภาคตัดขวางเชิงอนุพันธ์ เมื่อพลังงานสูงขึ้นความสูงของยอดจะเพิ่มขึ้นและความกว้างต่อมุมจะน้อยลง ซึ่งสอดคล้องกับผลการทดลองที่ผ่านมา



สถาบันวิทยบริการ
จุฬาลงกรณ์มหาวิทยาลัย

ภาควิชา ฟิสิกส์
สาขาวิชา ฟิสิกส์
ปีการศึกษา 2542

ลายมือชื่อนิสิต ..เสรี พงศ์พันธุ์ภาณี
ลายมือชื่ออาจารย์ที่ปรึกษา ..เดวิด รุฟไฟโโล
ลายมือชื่ออาจารย์ที่ปรึกษาร่วม ..วุฒิชัย พาราสุข

##3972289623 :MAJOR PHYSICS

KEYWORDS: ATOMIC PHYSICS / ATOMIC COLLISION / CHARGE TRANSFER / CROSS SECTION / DIFFERENTIAL CROSS SECTION / ATOMIC OXYGEN

SAREE PHONGPHANPHANEE: CHARGE TRANSFER OF O WITH H^+ AT HIGH TEMPERATURES. THESIS ADVISOR: ASSOC. PROF. DAVID RUFFOLO, Ph.D., THESIS COADVISOR: ASSOC. PROF. VUDHICHAI PARASUK, Ph.D., 65 pp. ISBN 974-334-042-4.

We are studying the theory of the charge transfer of atomic oxygen with a hydrogen ion in the velocity range of 400-800 km/s (0.18-0.36 a.u.). There are no previous calculations or experimental results for the differential cross section spanning this energy range. The quantum close-coupling and semi-classical methods were used in these calculations. Using previously published adiabatic potentials and nonadiabatic couplings, the results of cross sections from both methods are of the same order of magnitude as the previous calculations and experimental data. The differential cross sections from our quantal calculations have a peak value that increases with energy and an angular width that decreases with energy, as in previous experimental results.

ภาควิชา ฟิสิกส์
สาขาวิชา ฟิสิกส์
ปีการศึกษา 2542

ลายมือชื่อนิสิต ...
ลายมือชื่ออาจารย์ที่ปรึกษา ...
ลายมือชื่ออาจารย์ที่ปรึกษาร่วม ...



Acknowledgements

I would like to express my gratitude to so many people who have contributed to this thesis. I am grateful to all of them for their encouragement and support, especially Associate Professor Dr. David Ruffolo, my main advisor, Associate Professor Dr. Vudhichai Parasuk, my co-advisor, and Dr. Udomsilp Pinsuk for their useful advice, guidance and encouragement.

I would like to thank Mr. Paisan Tooprakai for computer assistance, and Miss Penphimon Ponsup, Miss Piyanate Chuychai, Miss Thiranee Khumlumlert, and Mr. Kobchai Tayanasanti for their help.

Finally, I would like to dedicate the thesis to my parents for their love.

สถาบันวิทยบริการ
จุฬาลงกรณ์มหาวิทยาลัย

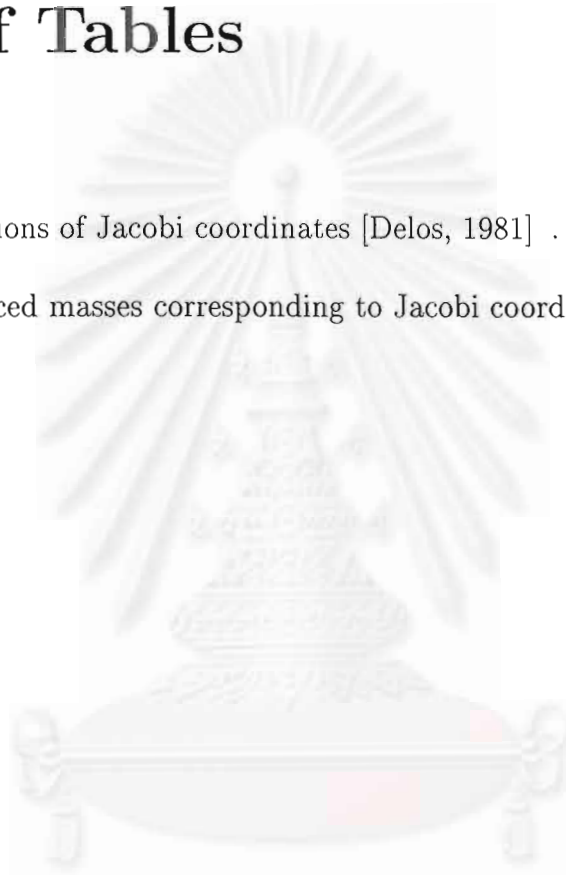
Contents

Abstract in Thai	iv
Abstract in English	v
Acknowledgements	vi
Table of Contents	vii
List of Tables	ix
List of Figures	x
1 Introduction	1
2 Theoretical Background	4
2.1 Quantum Mechanical Approach	5
2.1.1 Scattering Boundary Conditions	9
2.1.2 Perturbed Stationary States (PSS) and Coupled Equations	10
2.1.3 Improved Perturbed Stationary States	12

2.1.4	Many Electron Systems	17
2.2	Semi-classical approach	18
3	Numerical Methods	23
3.1	Log Derivative Method	23
3.2	Improved Log Derivative Method	27
3.3	Calculation Procedure	31
4	The Cross Section and Differential Cross Section of Charge Trans- fer between O and H ⁺	36
4.1	Quantal Calculations	40
4.2	Semi-classical Calculations	42
5	Conclusions	49
	References	51
	Appendices	
A	Various Forms of Switching Functions	56
B	Partial Wave Expansion	58
C	Program for Semi-classical Calculations	60
D	Program for Transforming an Adiabatic Potential to be Diabatic	66
	Curriculum Vitae	72

List of Tables

- | | | |
|-----|--|---|
| 2.1 | Relations of Jacobi coordinates [Delos, 1981] | 6 |
| 2.2 | Reduced masses corresponding to Jacobi coordinates [Delos, 1981] | 8 |



สถาบันวิทยบริการ
จุฬาลงกรณ์มหาวิทยาลัย

List of Figures

2.1	Jacobi coordinates of the system [Delos, 1981]	7
3.1	Flow chart of the calculation procedure.	33
3.2	Flow chart of the transformation from an adiabatic to a diabatic potential.	34
3.3	Flow chart of the semi-classical calculation procedure.	35
4.1	Adiabatic potentials of OH^+ [Kimura et al., 1997]. Blue lines are for $^3\Sigma^-$ states and red lines are for $^1\Pi$ states.	38
4.2	Coupling matrix elements [Kimura et al., 1997]	39
4.3	The differential cross section for charge transfer: Experimental results [Lindsay et al., 1996]	43
4.4	The differential cross section for charge transfer: Theoretical results [Hedström et al., 1998]	44
4.5	The differential cross section for charge transfer: Present calculations	45
4.6	The differential cross section for charge transfer: All results	46
4.7	The cross section for charge transfer	47

Chapter 1



Introduction

The charge exchange reaction from the collision of a proton and atomic oxygen is an important process for a wide range of physical situations.

In the Earth's atmosphere, about one hundred kilometers above the surface, atomic oxygen has a higher density than other species, such as N_2 and O_2 . Atomic oxygen is produced by the dissociation of O_2 by UV radiation. Then charge exchange between H^+ and atomic O is an important process in studying the Earth's atmosphere [Stebbing, 1964; Spjeldvik and Fritz, 1978; Spjeldvik, 1979; Schunk and Nagy, 1980; Picone et al., 1997; Michelis and Orsini, 1997].

Thermonuclear fusion involves a hot plasma. There are interactions between the hot plasma and the container wall, which may contain impurity ions, such as C, O and Fe. Although there is a small fraction of such ions the process of charge exchange is rapid and therefore important [Bransden, 1992; Janev et al., 1995].

In the astrophysics of determining the physical state of planetary nebulae, these objects have a low density hydrogen cloud around the central star. Atomic H ionized under the stellar radiation forms a plasma, and there are small amounts of neutral H and ions of other elements, such as C, N, O and Ne in various states of ionization. The charge exchange process is one process related to the study of nebulae [Péquiugnot, 1990].

In the solar system there is a type of cosmic rays, i.e., energetic particles, called anomalous cosmic rays. The charge exchange process helps determine the ionization of neutral atoms from the interstellar medium in the solar system, and such so-called pick-up ions can be accelerated at the solar wind termination shock at the edge of solar system to become anomalous cosmic rays [Stone et al., 1996; Lee, 1996].

The theoretical cross section of charge exchange of H^+ with O at 1000 K has been calculated by Field and Steigman [1971], using the orbiting approximation. A more rigorous calculation method was used for an energy corresponding to the same temperature by Chambaud et al. [1980], using molecular modeling with the spin orbit coupling interaction. Kimura et al. [1997] recently calculated the cross section in the energy range of 0.01 to 1.0 keV, using the “close coupling” method. The differential cross section and cross section at the overlapping energy range of 0.5, 1.0 and 5.0 keV was calculated by Hedström et al. [1998], using the electron nuclear dynamics method. The cross section in the energy range 0.1-100 keV was calculated by Hamre et al. [1999], using the simple model of the close

coupling method. Several of these works calculated the cross section, but there have been few studies of the differential cross section.

We want to calculate the cross section and differential cross section in the relative velocity range of solar wind speeds, 400-800 km/s (~ 0.18 - 0.36 a.u.). This range of speeds corresponds to the energy range of 0.8-3.4 keV or, using

$$E = kT, \quad (1.1)$$

to the temperature range of $0.9 \times 10^7 - 3.6 \times 10^7$ K, i.e., high temperatures. Only one previous study [Hedström et al. 1998] has examined the differential cross section in this velocity range, and that study only provided one point in this range (0.5 keV). Our results may be useful for studying anomalous cosmic rays and energetic neutral atoms in the heliosphere.

In this thesis, the theory of the close coupling and semi-classical methods for scattering is discussed in Chapter 2 and the numerical method is discussed in Chapter 3. Chapters 4 and 5 present the results and conclusions, respectively.

สถาบันวิทยบริการ
จุฬาลงกรณ์มหาวิทยาลัย

Chapter 2

Theoretical Background

For convenience we first consider the simplest charge transfer reaction: a system of one electron and two nuclei, i.e., the collision between H and H⁺. In this thesis, the system which is considered has a relative velocity that is slow compared with the electron velocity. The relative velocity of the system is equal to the solar wind speed, 400-800 km/s (0.18-0.36 in atomic units, a.u.). For atomic collisions with a relative velocity that is slow compared with the electron velocity, there are two types of methods that are commonly used: quantum mechanical and semi-classical (sometimes called “classical trajectory”). The former is expected to be much more accurate, given the theoretical approximations employed in the semi-classical formulation. In a quantum-mechanical scattering problem, the system is considered to be stationary in time, so we use the time-independent Schrödinger equation [Delos, 1981; Kimura and Lane, 1989; Brandsden and McDowell, 1992],

$$H(\vec{R}, \vec{r})\Psi(\vec{R}, \vec{r}) = E\Psi(\vec{R}, \vec{r}). \quad (2.1)$$

The Hamiltonian is

$$H(\vec{R}, \vec{r}) = T_N + h(\vec{R}, \vec{r}), \quad (2.2)$$

where T_N is the kinetic term of the nuclei in the center of mass frame,

$$T_N = -(2\mu)^{-1} \nabla_R^2, \quad (2.3)$$

μ is the reduced mass of the nuclei, and $h(\vec{R}, \vec{r})$ is the electronic Hamiltonian,

$$h(\vec{R}, \vec{r}) = -\frac{1}{2} \nabla_r^2 + V(\vec{R}, \vec{r}), \quad (2.4)$$

with $V(\vec{R}, \vec{r})$ as the total potential energy of the interaction between the electrons and nuclei. Here \vec{R} represents the internuclear vector and \vec{r} is the coordinate of the electron relative to the center of mass. Another way to solve the problem is semi-classical. In this viewpoint, the nuclei move classically along a fixed trajectory and the electron motion is quantum mechanical. The electronic wave function, $\Psi(\vec{r}, t)$, depends on time, so the time-dependent Schrödinger equation is used:

$$h(\vec{R}(t), \vec{r}) \Psi(\vec{r}, t) = i \frac{\partial}{\partial t} \Psi(\vec{r}, t). \quad (2.5)$$

2.1 Quantum Mechanical Approach

Consider the system of one electron and two nuclei with masses M_A and M_B , which have coordinates \vec{R}_A^0 and \vec{R}_B^0 , respectively, relative to a fixed laboratory origin, given by \vec{r}^0 . The case of many electrons will be considered at the end of this section. This is a three-body system, so the standard Jacobi coordinate

$$\lambda = (M_A - M_B)/(M_A + M_B)$$

$$\frac{1}{2}(1 + \lambda) = M_A/(M_A + M_B), \frac{1}{2}(1 - \lambda) = M_B/(M_A + M_B)$$

$$\vec{r} = \vec{r}_g + \frac{1}{2}\lambda\vec{R}$$

$$\vec{r}_A = \vec{r}_g + \frac{1}{2}\vec{R} = \vec{r} + \frac{1}{2}(1 - \lambda)\vec{R}$$

$$\vec{r}_B = \vec{r}_g - \frac{1}{2}\vec{R} = \vec{r} - \frac{1}{2}(1 + \lambda)\vec{R}$$

$$\vec{R}_A = \frac{M_A + \frac{1}{2}m_0}{M_A + m_0}\vec{R} - \frac{m_0}{M_A + m_0}\vec{r}_g$$

$$\vec{R}_A = \frac{M_A + \frac{1}{2}(1 + \lambda)m_0}{M_A + m_0}\vec{R} - \frac{m_0}{M_A + m_0}\vec{r}$$

$$\vec{R}_B = \frac{M_B + \frac{1}{2}m_0}{M_B + m_0}\vec{R} - \frac{m_0}{M_B + m_0}\vec{r}_g$$

$$\vec{R}_B = \frac{M_B + \frac{1}{2}(1 - \lambda)m_0}{M_B + m_0}\vec{R} - \frac{m_0}{M_B + m_0}\vec{r}$$

Table 2.1: Relations of Jacobi coordinates [Delos, 1981]

system will be used [Messiah, 1970]. These relations are shown in Table 2.1. The Schrödinger equation of the system is

$$H\Psi = (T + V)\Psi = E\Psi, \quad (2.6)$$

where Ψ is the wave function of the system. In Jacobi coordinates, T can be written as [Bransden, 1992]

$$T = -(2\mu_A)^{-1}\nabla_{R_A}^2 - (2m_A)^{-1}\nabla_{r_A}^2 \quad (2.7)$$

$$= -(2\mu_B)^{-1}\nabla_{R_B}^2 - (2m_B)^{-1}\nabla_{r_B}^2 \quad (2.8)$$

$$= -(2\mu)^{-1}\nabla_R^2 - (2m)^{-1}\nabla_r^2, \quad (2.9)$$

where the masses m and μ are defined in Table 2.2.

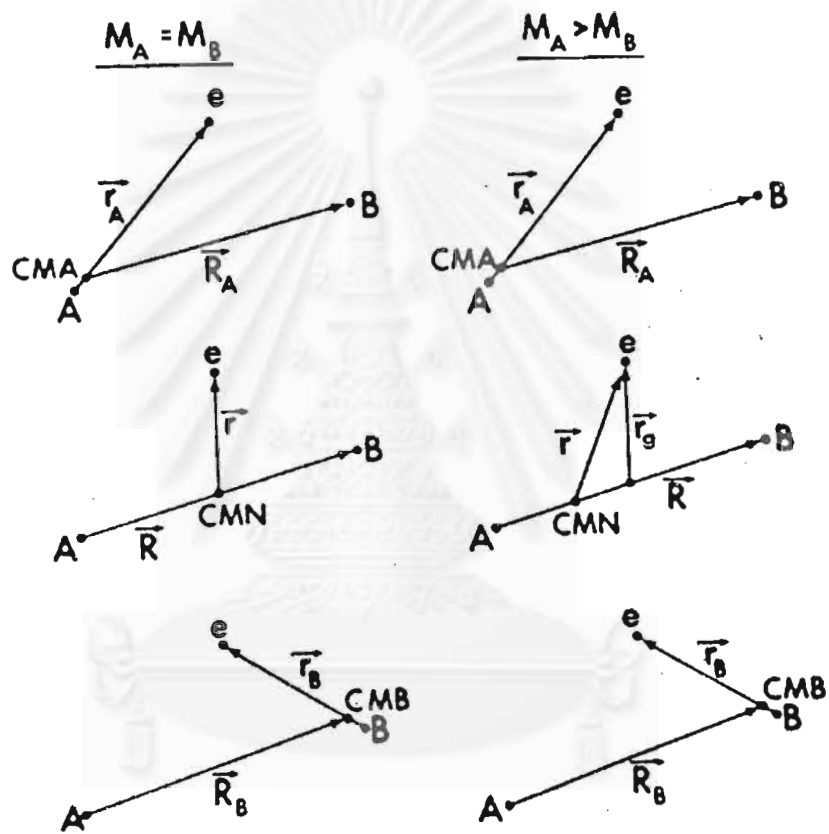


Figure 2.1: Jacobi coordinates of the system [Delos, 1981]

Coordinate	Reduced mass	
\vec{r}^0	m_0	Rest mass of electron (1 in atomic units)
\vec{R}_A^0	M_A	Rest mass of nucleus A
\vec{R}_B^0	M_B	Rest mass of nucleus B
\vec{R}_{CM}^0	$M_T = M_A + M_B + m_0$	Total mass of system
\vec{r}_A	$m_A = m_0 M_A / (m_0 + M_A)$	Electron reduced mass, channel A
\vec{R}_A	$\mu_A = (m_0 + M_A) M_B / M_T$	Nuclear reduced mass, channel A
\vec{r}_B	$m_B = m_0 M_B / (m_0 + M_B)$	Electron reduced mass, channel B
\vec{R}_B	$\mu_B = (m_0 + M_B) M_A / M_T$	Nuclear reduced mass, channel B
\vec{r}	$m = m_0 (M_A + M_B) / M_T$	Molecular electron reduced mass
\vec{R}	$\mu = M_A M_B / (M_A + M_B)$	Molecular nuclear reduced mass

Table 2.2: Reduced masses corresponding to Jacobi coordinates [Delos, 1981]

2.1.1 Scattering Boundary Conditions

The electron can be in 2 channels. Let channel A be the state of the electron which has an asymptotic probability density close to nucleus A when R_A goes to infinity. In that limit, the operator V of equation (2.6) then becomes the atomic potential of atom A, $V \rightarrow V_0^A(\vec{r}_A)$. The electronic Hamiltonian will be in the form

$$h_0^A = -(2m_A)^{-1}\nabla_{r_A}^2 + V_0^A(\vec{r}_A), \quad (2.10)$$

and the electronic wave functions are

$$h_0^A \phi_{n_A}^0 = \epsilon_{n_A}^0 \phi_{n_A}^0. \quad (2.11)$$

The channel wave number, k_{n_A} , is defined by

$$k_{n_A}^2/(2\mu_A) + \epsilon_{n_A}^0 = E. \quad (2.12)$$

Analogous quantities can be defined for channel B. Then the Hamiltonian can be separated into terms which depend on \vec{R}_A or \vec{r}_A ,

$$H \rightarrow (2\mu_A)^{-1}\nabla_{R_A}^2 - (2m_A)^{-1}\nabla_{r_A}^2 + V_0^A(\vec{r}_A).$$

The solution of the term which depends on \vec{R}_A corresponds to a free particle. Let the incident wave in channel A and initial state $\phi_{m_A}^0$ travel in direction Z_A . The asymptotic wave function for large R_A and finite r_A is [Delos, 1981]

$$\Psi \rightarrow \phi_{m_A}^0(\vec{r}_A) \exp(ik_{m_A}Z_A) + \sum_{n_A} \phi_{n_A}(\vec{r}_A) f_{n_A m_A}(\Theta_A, \Phi_A) \exp(ik_{n_A}R_A)/R_A, \quad (2.13)$$

while at large R_B and finite r_B ,

$$\Psi \rightarrow \sum_{n_B} \phi_{n_B}(\vec{r}_B) f_{n_B m_A}(\Theta_B, \Phi_B) \exp(ik_{n_B} R_B) / R_B, \quad (2.14)$$

where Φ_A, Φ_B, Θ_A , and Θ_B are spherical coordinates, Z_A is a Cartesian nuclear coordinate, and we define

$$\begin{aligned} \vec{R}_A &\rightarrow (X_A, Y_A, Z_A) \quad \text{or} \quad (R_A, \Theta_A, \Phi_A), \\ \vec{R}_B &\rightarrow (X_B, Y_B, Z_B) \quad \text{or} \quad (R_B, \Theta_B, \Phi_B), \\ \vec{R} &\rightarrow (X, Y, Z) \quad \text{or} \quad (R, \Theta, \Phi). \end{aligned}$$

2.1.2 Perturbed Stationary States (PSS) and Coupled Equations

In the Born-Oppenheimer approximation, when determining the electron dynamics we can neglect the motion of the nuclei and take them to be fixed. Then the electron dynamics is independent of the nuclear motion and the wave function can be separated between electronic and nuclear wave functions. We can expand the full wave function Ψ in terms of a linear combination of radial functions and electronic wave functions [Delos, 1981; Kimura, 1989],

$$\Psi(\vec{R}, \vec{r}) = \sum_n \chi_n(\vec{R}) \phi_n(\vec{r}; \vec{R}), \quad (2.15)$$

where $\phi_n(\vec{r}; \vec{R})$ is an eigenfunction of the electronic Hamiltonian for a given \vec{R} .

Putting the wave function from equation (2.15) into equation (2.6), and taking

the inner product with $\phi_m(\vec{r}; \vec{R})$, we obtain coupled equations for $\chi_n(\vec{R})$:

$$\{(2\mu)^{-1}[(-i\vec{\nabla})^2 + 2\vec{P}_{mn} \cdot (-i\vec{\nabla}) + B_{mn}^o] + h_{mn} - E\}\chi_n(\vec{R}) = 0. \quad (2.16)$$

where

$$\vec{P}_{mn} = \langle \phi_m | -i\vec{\nabla} | \phi_n \rangle$$

$$B_{mn}^o = \langle \phi_m | -\nabla^2 | \phi_n \rangle$$

$$h_{mn} = \langle \phi_m | h | \phi_n \rangle$$

Equation (2.16) can be written in another form by use of the assumption of a complete set [Delos, 1981],

$$B_{mn}^o = -i\vec{\nabla}_R \cdot \vec{P}_{mn} + \vec{P}_{ml} \cdot \vec{P}_{ln}, \quad (2.17)$$

so equation (2.16) becomes

$$\left[\frac{1}{2\mu} (-i\vec{\nabla} + \underline{\vec{P}})^2 + \underline{h} - E \right] \underline{\chi}(\vec{R}) = 0, \quad (2.18)$$

where underlined symbols indicate matrices in terms of m and n (symbols with both an arrow above and a line below are therefore third-ranked tensors).

Coupled equations of the form of equations (2.16) and (2.18) are used in many calculations of slow atomic collisions, but there are errors in these coupled equations. The most important problems are not satisfying boundary conditions and Galilean invariance. From equation (2.14), the wave function of channel A under asymptotic conditions should be

$$\Psi \rightarrow \exp(i\mu_A v Z_A) \phi_{n_A}^0(\vec{r}'_A) = \exp(i\mu v Z) \exp[-im^{\frac{1}{2}}(1-\lambda)vz'] \phi_{n_A}^0(\vec{r}'_A), \quad (2.19)$$

but the wave function in the asymptotic region which corresponds to equation (2.15) is

$$\Psi \rightarrow \exp(i\mu v Z) \phi_n(\vec{r}'; \vec{R}) \rightarrow \exp(i\mu v Z) \phi_{n_A}(\vec{r}'_A). \quad (2.20)$$

In equations (2.19) and (2.20), ϕ_{n_A} and $\phi_{n_A}^0$ should be the same in the asymptotic region, but the wave functions in these equations are different. The second exponential term in equation (2.19) is valid in equation (2.20).

The coupling matrix \vec{P} may not vanish at infinite range. For example, the radial component of the coupling matrix, \vec{P} , is

$$P_{mn}^r(R) = -i \langle \phi_m | \frac{\partial}{\partial R} | \phi_n \rangle. \quad (2.21)$$

This was first calculated for the H_2^+ system in 1960 [Jepsen and Hirschfelder, 1960] by using the Hellman-Feynman theorem to change it into a simple form,

$$P_{mn}^r(R) = \frac{-i \langle \phi_m | \frac{\partial \hbar}{\partial R} | \phi_n \rangle}{[\epsilon_n(R) - \epsilon_m(R)]}. \quad (2.22)$$

The result is not zero at large distances but it is constant. It is not correct because when the two atoms are far apart there is no charge exchange or other coupling. The other problems about PPS are i) unrealistic coupling between atoms in a symmetric molecule, and ii) it does not contain the momentum transfer factor. This error is corrected by the so-called electron translation factor (ETF).

2.1.3 Improved Perturbed Stationary States

We discussed in the above about the defects of PSS. The first correction of the defect was by using a plane wave translation factor [Bates and McCarroll, 1958;

cited by Delos, 1981], but at a low reaction velocity it is better to use a more complicated translation factor. Delos [1981] modified the PSS by using the reaction coordinate, $\vec{\xi}$, with the wave function expressed in the form,

$$\Psi = \sum_j \chi_j(\vec{\xi}_j) \phi_j(\vec{r}, \vec{\xi}_j), \quad (2.23)$$

where

$$\vec{\xi}_j = \vec{R} - \frac{\vec{w}_j}{\mu} \quad (2.24)$$

(for a dimensionless μ in atomic units) and

$$\vec{w}_j = \frac{1}{2} (f_j(\vec{r}, \vec{R}) + \lambda) \vec{r}_g + \frac{1}{8} (1 - \lambda^2) \vec{R}. \quad (2.25)$$

The function $f_j(\vec{r}, \vec{R})$ is called the switching function. The value of the switching function is between ± 1 and has these properties:

$$f_j(\vec{r}, \vec{R}) = \begin{cases} 1 & \text{as } R \rightarrow \infty \text{ and for } \vec{r}_B \ll \vec{r}_A \\ -1 & \text{as } R \rightarrow \infty \text{ and for } \vec{r}_A \ll \vec{r}_B \\ 0 & \text{as } R \rightarrow 0. \end{cases} \quad (2.26)$$

The reason a switching function with these properties is introduced is so that $\vec{\xi}_j \approx \vec{R}_A$ when the electron is close to A, and $\vec{\xi}_j \approx \vec{R}_B$ when the electron is close to B. Various forms of this switching function will be shown in Appendix A. The form of the coupled equation for $\chi_j(\vec{\xi}_j)$ can be found by substituting the wave function of equation (2.23) into the Schrödinger equation and taking the inner product with $\phi_i(\vec{r}, \vec{\xi}_i)$:

$$\sum_j \langle \phi_i(\vec{r}, \vec{\xi}_i) | H - E | \phi_j(\vec{r}, \vec{\xi}_j) \rangle \chi_j(\vec{\xi}_j) = 0. \quad (2.27)$$

We can evaluate the coupled equation by changing the variables H , \vec{r} and \vec{R} , to the reaction coordinates. Let a component of vector $\vec{\alpha}$ be denoted by α^a , where $a = x, y, z$ or X, Y, Z . Then we can transform the Hamiltonian by using the relation,

$$\left(\frac{\partial}{\partial R^a}\right)_{\vec{r}} = \left(\frac{\partial \xi^b}{\partial R^a}\right)_{\vec{r}} \left(\frac{\partial}{\partial \xi^b}\right)_{\vec{r}} \quad (2.28)$$

$$\left(\frac{\partial}{\partial r^a}\right)_{\vec{R}} = \left(\frac{\partial}{\partial r^a}\right)_{\vec{\xi}} + \left(\frac{\partial \xi^b}{\partial r^a}\right)_{\vec{R}} \left(\frac{\partial}{\partial \xi^b}\right)_{\vec{R}}. \quad (2.29)$$

Defining the new conjugate momenta of $(\vec{r}, \vec{\xi})$,

$$\begin{aligned} p^k &= -i \left(\frac{\partial}{\partial r^k}\right)_{\vec{\xi}} \\ P^k &= -i \left(\frac{\partial}{\partial \xi^k}\right)_{\vec{r}}, \end{aligned} \quad (2.30)$$

and

$$\begin{aligned} \Gamma_n^{ab}(\vec{r}, \vec{R})i &= \left(\frac{\partial w_n^b}{\partial R^a}\right)_{\vec{r}} \\ \gamma_n^{ab}(\vec{r}, \vec{R}) &= \left(\frac{\partial w_n^b}{\partial r^a}\right)_{\vec{R}}, \end{aligned} \quad (2.31)$$

the transformed Hamiltonian, $H(\vec{r}, \vec{R}) \rightarrow H(\vec{r}, \vec{\xi})$, is

$$\begin{aligned} H(\vec{r}, \vec{R}) &= -\frac{1}{2}\nabla_{\vec{r}}^2 - \frac{1}{2\mu}\nabla_{\vec{R}}^2 + V = H(\vec{r}, \vec{\xi}_n) \\ &= \frac{1}{2\mu} \left\{ P^a P^a + \frac{1}{2}(\gamma_n^{ab} P^b + P^b \gamma_n^{ab}) p^a + \frac{1}{2} p^a (\gamma_n^{ab} P^b + P^b \gamma_n^{ab}) \right. \\ &\quad + \frac{1}{\mu} \left[\frac{1}{4}(\gamma_n^{ab} P^b + P^b \gamma_n^{ab})(\gamma_n^{ac} P^c + P^c \gamma_n^{ac}) \right. \\ &\quad \left. \left. + \frac{1}{2}(\Gamma_n^{ab} P^b + P^b \Gamma_n^{ab}) P^a + \frac{1}{2} P^a (\Gamma_n^{ab} P^b + P^b \Gamma_n^{ab}) \right] \right\} \\ &\quad + \frac{1}{2} p^k p^k + V + O\left(\frac{1}{\mu^2}\right). \end{aligned} \quad (2.32)$$

We have neglected terms depending on $\nabla f/\mu$ which would appear in nuclear kinetic energy terms. Then the Hamiltonian can be simplified to become

$$\begin{aligned}
H = & \frac{1}{2\mu} \left\{ P^a P^a + \frac{1}{2} (\gamma_n^{ab} P^b + P^b \gamma_n^{ab}) p^a \right. \\
& + \frac{1}{2} p^a (\gamma_n^{ab} P^b + P^b \gamma_n^{ab}) \\
& + \frac{1}{\mu} (\gamma_n^{ab} \gamma_n^{ac} + 2\delta_{ac} \Gamma_n^{ab}) P^b P^c \left. \right\} \\
& + \frac{1}{2} p^a p^a + V(\vec{r}, \vec{\xi}_n). \tag{2.33}
\end{aligned}$$

Thronson and Delos [1978] discussed how the terms of the coupled equation can be reduced and given by

$$[(2\mu)^{-1}(-i\vec{\nabla} + \vec{P} + \vec{A})^2 + \underline{h} - E]\underline{\chi}(\vec{R}) = 0, \tag{2.34}$$

where

$$A_{ij}(\xi_n) = -i\langle \phi_i | \{ \vec{\nabla}_r(\vec{w}_n) \cdot \vec{\nabla}_r + \frac{1}{2} \vec{\nabla}^2(\vec{w}_n) \} | \phi_j \rangle. \tag{2.35}$$

The form of equation (2.34) is same as that of equation (2.16). Matrix \vec{A} is a correction to matrix \vec{P} .

In this thesis we will show the solution of a system which has only radial parts of matrices $\vec{P} + \vec{A}$. Then in equation (2.34), the potential, coupling and potential energy terms do not depend on the angle. By using spherical harmonics in the expansion of the wave function, we can write

$$\left\{ \frac{1}{2\mu} \left[-i\frac{\partial}{\partial R} + (\underline{P}^R + \underline{A}^R) \right]^2 + \frac{l(l+1)}{2\mu R^2} + \underline{h} - E \right\} \underline{F}(R) = 0. \tag{2.36}$$

The representation of the above is called an adiabatic representation. It is more convenient to calculate this in the form of a diabatic representation. Diabatic

means that the radial coupling vanishes: $\underline{P}^R + \underline{A}^R = 0$ [Delos, 1981]. Then we can transform to diabatic form by using a transformation matrix, \underline{C} , which satisfies [Smith, 1969]

$$\underline{P}(R)\underline{C}(R) + i\frac{\partial}{\partial R}\underline{C} = 0, \quad (2.37)$$

where here we use $\underline{P} = \underline{P}^R + \underline{A}^R$. Then the transformation matrix, \underline{C} , is the solution of the integral equation

$$\underline{C}(R) = \underline{I} + i \int_R^\infty \underline{P}(R')\underline{C}(R')dR', \quad (2.38)$$

which can be solved by use of an iteration method:

$$\begin{aligned} \underline{C}(R) = & \underline{I} + i \int_R^\infty \underline{P}(R')dR' \\ & + (i)^2 \int_R^\infty \underline{P}(R') \int_{R'}^\infty \underline{P}(R'')dR''dR' + \dots \end{aligned} \quad (2.39)$$

Then the coupled equation (2.34) becomes

$$\left(-\frac{\partial^2}{\partial R^2} + \underline{V}^d(R) \right) \underline{F}(R) = 0, \quad (2.40)$$

where V^d is the diabatic potential,

$$\underline{V}^d(R) = \underline{C}^\dagger(R)\underline{V}^{ad}(R)\underline{C}(R), \quad (2.41)$$

where

$$\underline{V}^{ad}(R) = \underline{I} \left[\hbar - 2\mu E + \frac{l(l+1)}{R^2} \right]. \quad (2.42)$$

In the adiabatic representation there are avoided crossings of potential curves, but after transformation to the diabatic representation crossings can occur. The numerical methods for solving the coupled equation will be shown in Chapter 3.

2.1.4 Many Electron Systems

The formulae above were based on a one electron system. However, there are many systems that have many electrons, so the formulae have to be modified for many electron systems. Whereas in the above section the wave function depended on one electron coordinate and multiple nuclear coordinates, in the many electron system the wave function must depend on all electron coordinates and nuclear coordinates,

$$\Psi(\vec{r}_1, \vec{r}_2, \vec{r}_3, \dots, \vec{R}), \quad (2.43)$$

where \vec{r}_i is the coordinate of each electron.

In this case, the solution of the problem is qualitatively similar, but the calculation of the coupling terms is more complicated and there are other minor complications which we do not go into here. For details, the reader is referred to Delos [1981] and Bransden and McDowell [1992].

The many electron wave function was used in calculating adiabatic potentials, h_{ii} , and non-adiabatic matrix elements, $(\vec{P} + \vec{A})_{ij}$. In this work we do not need to use the many electron wave function in calculations, because the many electron wave function was taken into account in the adiabatic potentials and non-adiabatic coupling matrix elements.

2.2 Semi-classical approach

Consider the system of one electron and two nuclei, A and B. In the semi-classical approach, the nuclei are considered to move along a classical path due to the nucleus-nucleus interaction (repulsion), and the electron dynamics use quantum mechanics. The internuclear distance depends on time, $\vec{R}(t)$, and the electronic wave function satisfies the time-dependent Schrödinger equation,

$$i\frac{\partial\Psi(\vec{r}, t)}{\partial t} = h\Psi(\vec{r}, t) \quad (2.44)$$

where Ψ and h are the electronic wave function and electronic Hamiltonian, respectively, and coordinates are defined as in Section 1. A further approximation, the straight-line approximation [Delos, 1981; Kimura and Lane, 1989; Bransden and McDowell, 1992], takes the trajectory to be the straight line, $\vec{R} = \vec{b} + \vec{v}t$, where $\vec{b} \perp \vec{v}$. As in the quantum mechanical method, when using \vec{R} and \vec{r} , there are problems regarding Galilean invariance and satisfying boundary conditions [Delos, 1981; Kimura and Lane, 1989]. To solve these problems, the electron transfer function (ETF) can also be included in this method.

We expand the wave function in the form [Kimura and Lane, 1989]

$$\Psi(\vec{r}, t) = \sum_i a_i(t)\phi_i(\vec{R}(t), \vec{r})F_i(R(t), \vec{r}), \quad (2.45)$$

where the term F_i comes from the electron translation factor, and can be written as

$$F_i = \exp[i\vec{v} \cdot \vec{w}_n(\vec{r}, \vec{R})]. \quad (2.46)$$

Inserting equation (2.45) into the time-dependent Schrödinger equation, and keeping terms only to first order in \vec{v} , then we get the coupled equation,

$$i \frac{d\mathbf{a}}{dt} = [\underline{h} + \vec{v} \cdot (\vec{P} + \vec{A})] \mathbf{a}. \quad (2.47)$$

where matrices \vec{P} and \vec{A} are defined as in the previous section.

The total cross section can be calculated from the asymptotic transition probability as a function of the impact parameter, $P(b)$, where the transition probability is the square of the amplitude at infinity, a_{ij} :

$$P_{ij}(b) = |a_{ij}(b, t \rightarrow \infty)|^2, \quad (2.48)$$

and the subscripts ij refer to initial and final states, respectively. The total cross section of scattering can be calculated from the integral of the impact parameter times the transition probability over the impact parameter,

$$\sigma_{ij} = 2\pi \int_0^\infty b P_{ij}(b) db. \quad (2.49)$$

The differential cross section normally calculated from the deflection function $\Theta(b)$ and the corresponding differential cross section is [Bransden and McDowell, 1992]

$$\frac{d\sigma_{ij}}{d\Omega} = \frac{bdb}{\sin \Theta d\Theta} P_{ij}(b). \quad (2.50)$$

However, in the straight line approximation, we do not have the deflection function. Instead, the differential can be calculated from a formula found from the eikonal approximation. The differential cross section from the eikonal approximation is obtained by starting with the standard scattering amplitude [Bransden

and McDowell, 1992],

$$f_{ij}(\Theta, \Phi) = -\frac{\mu}{2\pi} \int d^3r \int d^3R \Phi_j^*(\vec{r}, \vec{R}) V_j(\vec{r}, \vec{R}) \Psi_i(\vec{r}, \vec{R}), \quad (2.51)$$

where Ψ_i is a total wave function corresponding to the state in which the incident wave is in channel i , Φ_j is the unperturbed scattered wave which is asymptotically in channel j , and V_j is the perturbation. The unperturbed wave function, Φ , satisfies the equation,

$$(h - V_j)\Phi = \Phi. \quad (2.52)$$

For the electron transfer to be system A, ($A+e^-$), V_j is

$$V_j = V_{Be} + V_{AB}, \quad (2.53)$$

where V_{Be} is the interaction potential between nucleus B and the electron, and V_{AB} is the interaction between A and B. The wave function $\Psi_i(\vec{r}, \vec{R})$ can be expressed in the form [Bransden and McDowell, 1992],

$$\Psi_i(\vec{r}, \vec{R}) = F_i(\vec{R}) \psi_i(\vec{r}, t). \quad (2.54)$$

In the straight-line approximation we can approximate $F_i(\vec{R})$ as a plane wave,

$$F_i(\vec{R}) = \exp(i\vec{K}_i \cdot \vec{R}), \quad (2.55)$$

where \vec{K}_i is along the incident direction and $K_i = \mu v_0$. The scattered wave Φ_j is also the product of a plane wave and the asymptotic wave function of equation (2.44),

$$\Phi_j(\vec{r}, \vec{R}) = \exp(i\vec{K}_j \cdot \vec{R}) \psi_j(\vec{r}, t), \quad (2.56)$$

where \vec{K}_j is along the scattering direction, (Θ, Φ) , and $|\vec{K}_i| = |\vec{K}_j|$. From the trajectory $\vec{R} = \vec{v}_0 t + \vec{b}$, and $\vec{v}_0 \perp \vec{b}$, then

$$d\vec{R} = v_0 d^2 b dt. \quad (2.57)$$

Using equations (2.51), (2.55), and (2.56), the scattering amplitude becomes

$$f_{ij}(\Theta, \Phi) = -\frac{\mu v_0}{2\pi} \int_{-\infty}^{+\infty} dt \int d^2 b \exp[i(\vec{K}_i - \vec{K}_j) \cdot \vec{R}] \langle \psi_j | V | \psi_i \rangle. \quad (2.58)$$

For small angle scattering we can approximate

$$(\vec{K}_i - \vec{K}_j) \cdot \vec{R} \approx \vec{K} \cdot \vec{b} \quad (2.59)$$

where the \vec{K} has the magnitude,

$$K = |\vec{K}_i - \vec{K}_j| = 2\mu v_0 \sin \frac{\Theta}{2}. \quad (2.60)$$

Using equation (2.58) and (2.59), then

$$f_{ij}(\Theta, \Phi) = -\frac{\mu v_0}{2\pi} \int_{-\infty}^{+\infty} dt \int d^2 b \exp(i\vec{K} \cdot \vec{b}) \langle \psi_j | V | \psi_i \rangle. \quad (2.61)$$

This expression can be reduced by using the relation,

$$V_j \psi_j = \left(h - i \frac{\partial}{\partial t} \right) \psi_j. \quad (2.62)$$

Integrating equation (2.61) by parts, and because h is Hermitian, equation (2.61)

becomes

$$\begin{aligned} f_{ij}(\Theta, \Phi) &= -\frac{i\mu v_0}{2\pi} \int d^2 b \exp(i\vec{K} \cdot \vec{b}) \langle \psi_j(\vec{r}, t) | \psi_i(\vec{r}, t) \rangle \Big|_{t=-\infty}^{t=+\infty} \\ &= -\frac{i\mu v_0}{2\pi} \int d^2 b \exp(i\vec{K} \cdot \vec{b}) a_{ij}(\vec{b}, t = +\infty) \end{aligned} \quad (2.63)$$

In two dimensions the parameter \vec{b} lies in a plane normal to the incident direction, and the direction in the plane can be defined by an azimuthal angle, ϕ_b . The amplitude $a_{ij}(\vec{b})$ of the reaction of scattering in which the initial state has magnetic quantum number m_i and the final state has magnetic quantum number m_j can be written as [Bransden and McDowell, 1992]

$$a_{ij}(\vec{b}) = a_{ij}(b) \exp[i(m_i - m_j)\phi_b], \quad (2.64)$$

where $a_{ij}(b)$ is independent of the azimuthal angle ϕ_b . Let the direction of incidence be along the z -axis and let the x -axis be along the scattering plane. For small angle scattering, \vec{K} lies in the xy plane in a direction specified by Φ , the azimuthal angle, so this is also the angle of \vec{K}_j . The angle between \vec{K} and \vec{b} is $(\Phi - \phi_b)$, so that

$$\vec{K} \cdot \vec{b} = kb \cos(\Phi - \phi_b). \quad (2.65)$$

From a property of Bessel functions,

$$\frac{1}{2\pi} \int_0^{2\pi} \exp(-in\phi_b + ix \sin \phi_b) d\phi_b = J_n(x). \quad (2.66)$$

Using equations (2.64), (2.65), and (2.66), then equation (2.63) becomes

$$f_{ij}(\Theta, \Phi) = i\mu v_0 \exp(-i\Delta m \Phi) (i)^{\Delta m} \int_0^{+\infty} b db J_{\Delta m}(2\mu v_0 b \sin \frac{\Theta}{2}) a(b, t = \infty) \quad (2.67)$$

The differential cross section of scattering from the state i to state j is the square of the scattering amplitude, $f_{ij}(\Theta, \Phi)$:

$$\frac{d\sigma_{ij}}{d\Omega} = |f_{ij}(\Theta, \Phi)|^2. \quad (2.68)$$

Chapter 3

Numerical Methods

There are various methods for solving the quantal coupled equations for scattering. The most famous methods are Gordon's method and the log derivative method. Others are the finite element and equivalent integral equations methods. In this thesis the log derivative method was used. We study only open channel systems, where "open channel" means that the total energy is higher than the potential; if the total energy is lower we call it a closed channel. The log derivative method is presented in Section 3.1 and the modified log derivative method in Section 3.2.

3.1 Log Derivative Method

The log derivative method for solving the scattering close-coupling matrix equation was constructed by Johnson [1973]. The matrix coupling equation in the last

chapter can be written in the form

$$\left(\frac{d^2}{dR^2}\underline{\mathbb{I}} - \underline{\mathbb{V}}\right)\underline{\Phi}(R) = 0. \quad (3.1)$$

Here $\underline{\mathbb{V}}$ is a symmetric potential matrix that includes the coupling matrix, potential energy and angular momentum term, $\underline{\mathbb{V}} = (-E + l(l+1)/R^2)\underline{\mathbb{I}} + \underline{\mathbb{V}}^d$. In index notation, V_{mn} represents the overlap between channel m and channel n . The wave function $\underline{\Phi}$ is a square matrix, where each column represents a linearly independent solution, or each element Φ_{ij} indicates the amplitude of the scattered wave of state j , given an initial state i . The log derivative is defined by

$$\underline{\mathbb{Y}}(R) = \underline{\Phi}'(R)\underline{\Phi}^{-1}(R). \quad (3.2)$$

By differentiating equation (3.2) and eliminating the second derivative term in equation (3.1), we obtain the matrix Ricatti equation,

$$\underline{\mathbb{Y}}'(R) = \underline{\mathbb{V}}(R) - \underline{\mathbb{Y}}^2. \quad (3.3)$$

Thus the second-order equation reduces to a first-order equation. In the scattering problem we are interested in the value at large distances, so we want to know $\underline{\Phi}$ at infinity. At the other boundary, $R = 0$, $\underline{\Phi}(0) = 0$, because of the infinite Coulomb barrier there. The inverse of the wave function becomes infinite, $\underline{\Phi}^{-1}(0) = \infty$, so the log derivative becomes infinite, $\underline{\mathbb{Y}}(0) = \infty$, Then $\underline{\mathbb{Y}}$ is taken to be a diagonal matrix with large elements.

Johnson's algorithm for numerically solving the equation is

$$\underline{\mathbb{Y}}_{n+1} = (\underline{\mathbb{I}} + h\underline{\mathbb{Y}}_n)^{-1}\underline{\mathbb{Y}}_n + (h/3)\omega_n\underline{\mathbb{U}}_n, \quad (3.4)$$

where $R_n = R_0 + nh$, $\underline{Y}(R_n)$ is the exact value, \underline{Y}_n is the approximate value computed by this method, $\underline{Y}_n \approx \underline{Y}(R_n)$, h is the spacing between integration points, and

$$\underline{U}_n = \begin{cases} \underline{Y}(R_n), & n = 0, 2, 4, \dots, N, \\ [\underline{I} + (h^2/6)\underline{Y}(R_n)]^{-1} \underline{Y}(R_n), & n = 1, 3, 5, \dots, N-1. \end{cases} \quad (3.5)$$

The weights, w_n , are the same as in the Simpson integration rule,

$$w_n = \begin{cases} 1, & n = 0, N, \\ 4, & n = 1, 3, 5, \dots, N-1, \\ 2, & n = 2, 4, 6, \dots, N-2. \end{cases} \quad (3.6)$$

The first term of the right hand side of equation (3.4) comes from estimating the term $-\underline{Y}^2$ in equation (3.3) at the midpoint, $n + \frac{1}{2}$, as approximately $-\underline{Y}_{n+1}\underline{Y}_n$. If we consider the effect of this term alone, we then have

$$\begin{aligned} \underline{Y}_{n+1} &= \underline{Y}_n - h\underline{Y}_{n+1}\underline{Y}_n \\ \underline{Y}_{n+1} &= (\underline{I} + h\underline{Y}_n)^{-1}\underline{Y}_n. \end{aligned} \quad (3.7)$$

This explains the first term on the right hand side of equation (3.4), and the second term comes from the modified Simpson's rule [Secret and Johnson, 1966]. The number of integration points must be odd, and the error of integration is

$$\underline{Y}(R_n) = \underline{Y}_n + \underline{C}h^4 + \underline{O}(h^6), \quad (3.8)$$

where \underline{C} is some unknown constant matrix, and $\underline{O}(h^6)$ is a matrix of order h^6 . If we consider of R_N to be a large distance of integration, then $\Phi(R_N)$ is the final

solution. For convenience we let $\underline{Z} = h\underline{Y}$, so equation (3.4) becomes

$$\underline{Z}_{n+1} = (\underline{I} + \underline{Z}_n)^{-1}\underline{Z}_n + (h^2/3)w_n\underline{U}_n. \quad (3.9)$$

The initial value at the classical turning point is

$$\underline{Y}_0 = 10^{20}\underline{I},$$

$$\underline{Z}_0 = 10^{20}\underline{I}.$$

The wave function at asymptotic distances, $R \geq R_N$, can be written in terms of a reaction matrix (\underline{K}):

$$\underline{\Phi}(R) = \underline{J}(R) + \underline{N}(R)\underline{K} \quad (3.10)$$

where the matrices are diagonal, and matrix elements of the open channel are the Ricatti-Bessel functions,

$$\underline{J}(R)_{ij} = \delta_{ij}k_j^{-1/2}j_l(k_jR), \quad (3.11)$$

$$\underline{N}(R)_{ij} = \delta_{ij}k_j^{-1/2}n_l(k_jR), \quad (3.12)$$

and k_j is the wave number channel. Differentiating $\underline{\Phi}(R)$ in equation (3.10) with respect to R , and multiplying with its inverse, then the matrix \underline{K} can be written in the form

$$\begin{aligned} \underline{Y} &= [\underline{J}'(R) + \underline{N}'(R)\underline{K}][\underline{J}(R) + \underline{N}(R)\underline{K}]^{-1} \\ \underline{K} &= -[\underline{Y}(R)\underline{N}(R) - \underline{N}'(R)]^{-1} \times [\underline{Y}(R)\underline{J}(R) - \underline{J}'(R)]. \end{aligned} \quad (3.13)$$

The \underline{S} matrix can be calculated from \underline{K} by the relation,

$$\underline{S} = (\underline{I} + i\underline{K})^{-1}(\underline{I} - i\underline{K}). \quad (3.14)$$

The total and differential cross sections can be calculated from the scattering matrix \underline{S} by using formulas given in Appendix B.

3.2 Improved Log Derivative Method

Manolopoulos [1986] further developed Johnson's algorithm. The reference potential was added to the original method, and it improved the convergence of this method with respect to the number of grid points.

Starting as in Johnson's method, the log derivative was defined as in equation (3.2). The log derivative matrix is undefined when the determinant vanishes, and such a singularity prohibits the standard numerical solution of equation (3.1). Manolopoulos introduced an imbedding-type propagator, \underline{Y} , which was defined on an interval $[R_1, R_2]$ by

$$\begin{bmatrix} \underline{\Phi}'(R_1) \\ \underline{\Phi}'(R_2) \end{bmatrix} = \begin{bmatrix} \underline{Y}_1(R_1, R_2) & \underline{Y}_2(R_1, R_2) \\ \underline{Y}_3(R_1, R_2) & \underline{Y}_4(R_1, R_2) \end{bmatrix} \begin{bmatrix} -\underline{\Phi}(R_1) \\ \underline{\Phi}(R_2) \end{bmatrix}. \quad (3.15)$$

The propagator matrix is obtained by solving the appropriate boundary value problem on the interval $[R_1, R_2]$. Multiplying the first equations of equation (3.15) through by $\Phi^{-1}(R_1)$ and the second by $\Phi^{-1}(R_2)$ and eliminating $\Phi(R_1)\Phi^{-1}(R_2)$, then the relation of the log derivative is

$$\begin{aligned} \underline{Y}(R_2) &= \underline{Y}_4(R_1, R_2) - \underline{Y}_3(R_1, R_2) \\ &\times [\underline{Y}(R_1) + \underline{Y}_1(R_1, R_2)]^{-1} \underline{Y}_2(R_1, R_2). \end{aligned} \quad (3.16)$$

Let the log derivative matrix propagate in the interval $[a, b]$. In the interval $[a, b]$ divided into two half-sections, define the midpoint point c and half step h by

$$\begin{aligned} c &= \frac{a+b}{2}, \\ h &= \frac{b-a}{2}. \end{aligned} \quad (3.17)$$

The region $[R_1, R_2]$ will denote both half-intervals. The homogeneous problem can be constructed on the interval $[a, b]$ in the form

$$\underline{\Psi}''(R) = \underline{V}_{\text{ref}}(R)\underline{\Psi}(R), \quad (3.18)$$

where $\underline{\Psi}$ is the homogeneous solution and the reference potential $\underline{V}_{\text{ref}}(R)$ is continuous throughout the sector. In the Johnson method the reference potential is zero, but in this method the reference potential is the piecewise constant matrix,

$$\underline{V}_{\text{ref}}(R)_{ij} = \delta_{ij}p_j^2, \quad R \in [a, b], \quad (3.19)$$

where p_j is constant in the interval. For this reference potential is not difficult to solve the homogeneous solution analytically. The propagator matrix, \underline{y} , which corresponds to homogeneous solutions, is defined by

$$y_1(R_1, R_2)_{ij} = y_4(R_1, R_2)_{ij} = \delta_{ij} \begin{cases} |p_j| \coth |p_j|h, & p_j^2 \geq 0 \\ |p_j| \cot |p_j|h, & p_j^2 < 0 \end{cases} \quad (3.20)$$

$$y_2(R_1, R_2)_{ij} = y_3(R', R'')_{ij} = \delta_{ij} \begin{cases} |p_j| \operatorname{csch} |p_j|h, & p_j^2 \geq 0 \\ |p_j| \operatorname{csc} |p_j|h, & p_j^2 < 0. \end{cases} \quad (3.21)$$

These propagators are undefined when the argument $|p_j|/h$ equals an integer multiple of π . However, we use a small step size so this event will not occur.

We define the potential matrix to be

$$\underline{U}(R) = \underline{V}(R) - \underline{V}_{\text{ref}}(R), \quad (3.22)$$

and use the same quadrature as in Johnson [1973]. Then we get the quadrature contribution from the tree grid point interval $[a, b]$ given by,

$$\begin{aligned} \underline{Q}(a) &= \frac{h}{3} \underline{U}(a), \\ \underline{Q}(c) &= \frac{1}{2} \left[\underline{I} - \frac{h^2}{6} \underline{U}(c) \right]^{-1} \frac{4h}{3} \underline{U}(c) \\ &= \frac{4}{h} \left[\underline{I} - \frac{h^2}{6} \underline{U}(c) \right]^{-1} - \frac{4}{h} \underline{I} \\ \underline{Q}(b) &= \frac{h}{3} \underline{U}(b). \end{aligned} \quad (3.23)$$

The quadrature contribution will be the same as quadrature in Johnson's method when the reference potential is zero. The effective half-interval propagator of the solution of equation (3.1) was defined by $\hat{\underline{Y}}$. It included the effect of the reference potential and residual potential, so we can write the effective half-interval propagator in the form,

$$\begin{aligned} \hat{\underline{Y}}_1(R_1, R_2) &= y_1(R_1, R_2) + Q(R_1), \\ \hat{\underline{Y}}_2(R_1, R_2) &= y_2(R_1, R_2), \\ \hat{\underline{Y}}_3(R_1, R_2) &= y_3(R_1, R_2), \\ \hat{\underline{Y}}_4(R_1, R_2) &= y_4(R_1, R_2) + Q(R_2). \end{aligned} \quad (3.24)$$

The log derivative matrix is propagated across the interval from a to b by the effective propagator. Thus the log derivative matrix can be derived as

$$\begin{aligned}\hat{\underline{Y}}(R_2) &= \hat{\underline{Y}}_4(R_1, R_2) - \hat{\underline{Y}}_3(R_1, R_2) \\ &\times [\hat{\underline{Y}}(R_1) + \hat{\underline{Y}}_1(R_1, R_2)]^{-1} \hat{\underline{Y}}_2(R_1, R_2).\end{aligned}\quad (3.25)$$

where

$$\hat{\underline{Y}}(a) = \underline{Y}(a), \quad (3.26)$$

and

$$\hat{\underline{Y}}(b) = \underline{Y}(b) + O(h^4). \quad (3.27)$$

Manolopoulos [1986] used a constant in the reference potential equal to diagonal elements of the potential matrix at the midpoint of the interval,

$$p_j^2 = V(c)_{jj}. \quad (3.28)$$

This choice can improve the convergence from Johnson's method.

For the log derivative propagating in the interval $[r_{\min}, r_{\max}]$, the radial wave function can be approximated to be zero, and the WKB method can be used to initialize the log derivative matrix, so it can be written as a diagonal matrix,

$$Y(R_{\min})_{ij} = \delta_{ij} V(R_{\min})_{ij}^{1/2} \quad (3.29)$$

The log derivative matrix at $r = r_{\max}$ can be calculated for the \underline{K} matrix by the same method as in Section 3.1.

3.3 Calculation Procedure

In this thesis the quantal calculations start with previously published adiabatic potentials and non-adiabatic coupling matrix elements [Kimura et al. 1997], followed by the transformation from adiabatic to diabatic potentials. The coupling equation (3.1) was solved by the method of Manolopoulos [1986]. The log derivative matrix in the asymptotic limit was calculated, and the K, S, and T matrices were calculated from equations (3.13), (3.14) and (B.7). The cross section and differential cross section were calculated from the T matrix by using formulae in Appendix B.

The semi-classical calculations start with equation (2.47), which is solved by using 4th-order Runge-Kutta method. The amplitude, $a_{ij}(b, t = \infty)$, was calculated. The cross section can be calculated by integrating $2\pi|a_{ij}(b, t = \infty)|^2$ over the impact parameter, b .

The flow chart of both quantal and semi-classical calculations is shown in Figure 3.1. The program `quantxs` from R. J. Allen, from <http://wserv1.dl.ac.uk/CCP/CCP6/quantx/>, was used for solving the coupled equations and calculating differential and total cross sections. Figure 3.2 shows the flow chart for a program written for this thesis, in order to transform potentials from adiabatic to diabatic form, which is a necessary step before using the `quantxs` program. The source code is presented in Appendix C. Semi-classical calculations were performed according to the flow chart in Figure 3.3. The source

code for this is presented in Appendix D.



สถาบันวิทยบริการ
จุฬาลงกรณ์มหาวิทยาลัย

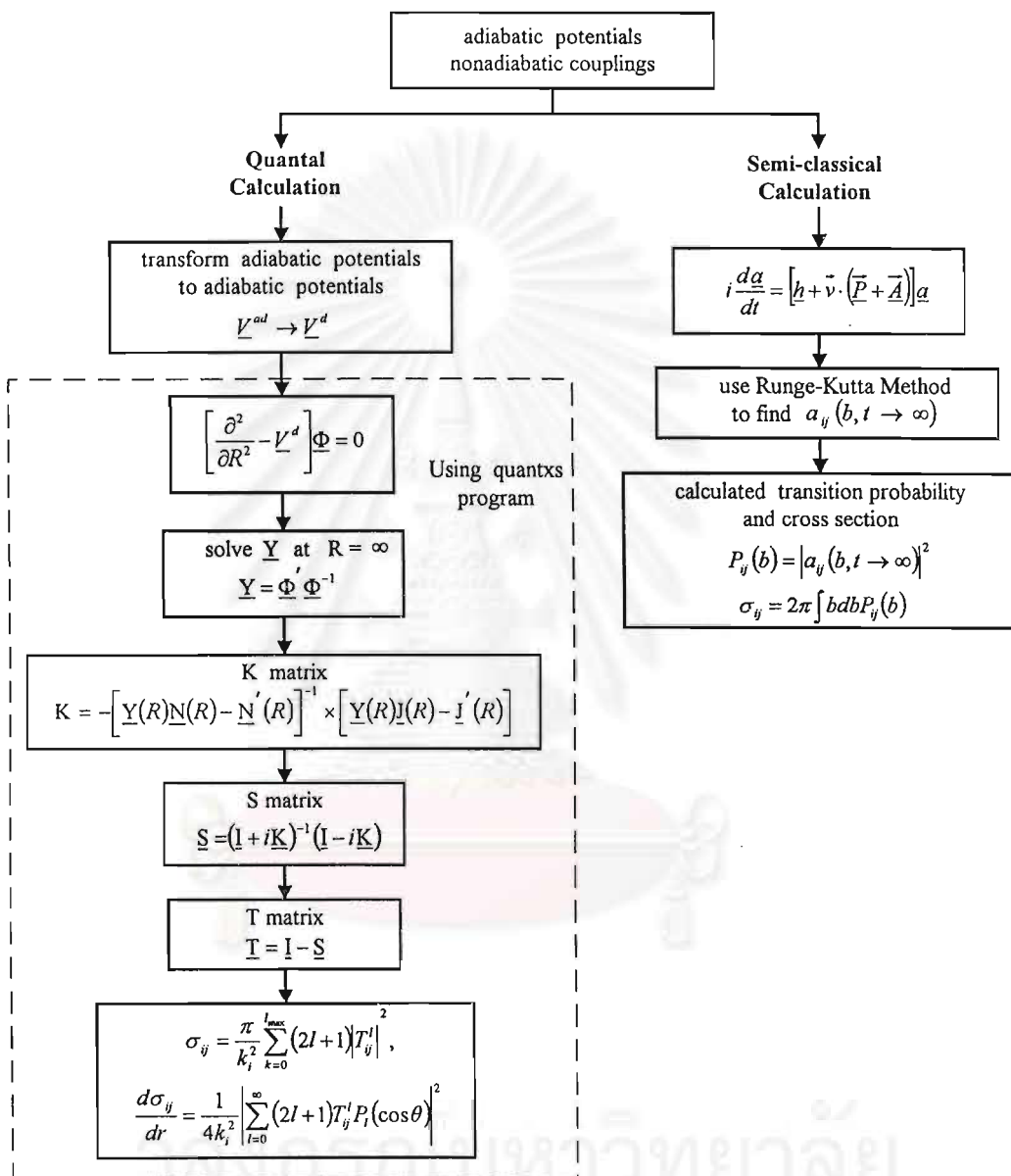


Figure 3.1: Flow chart of the calculation procedure.

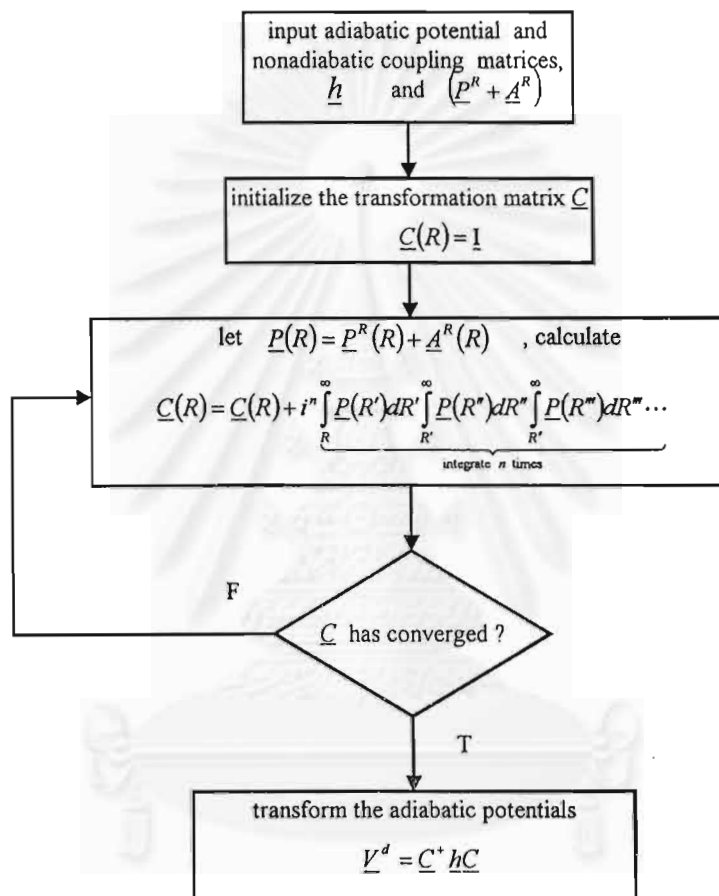


Figure 3.2: Flow chart of the transformation from an adiabatic to a diabatic potential.

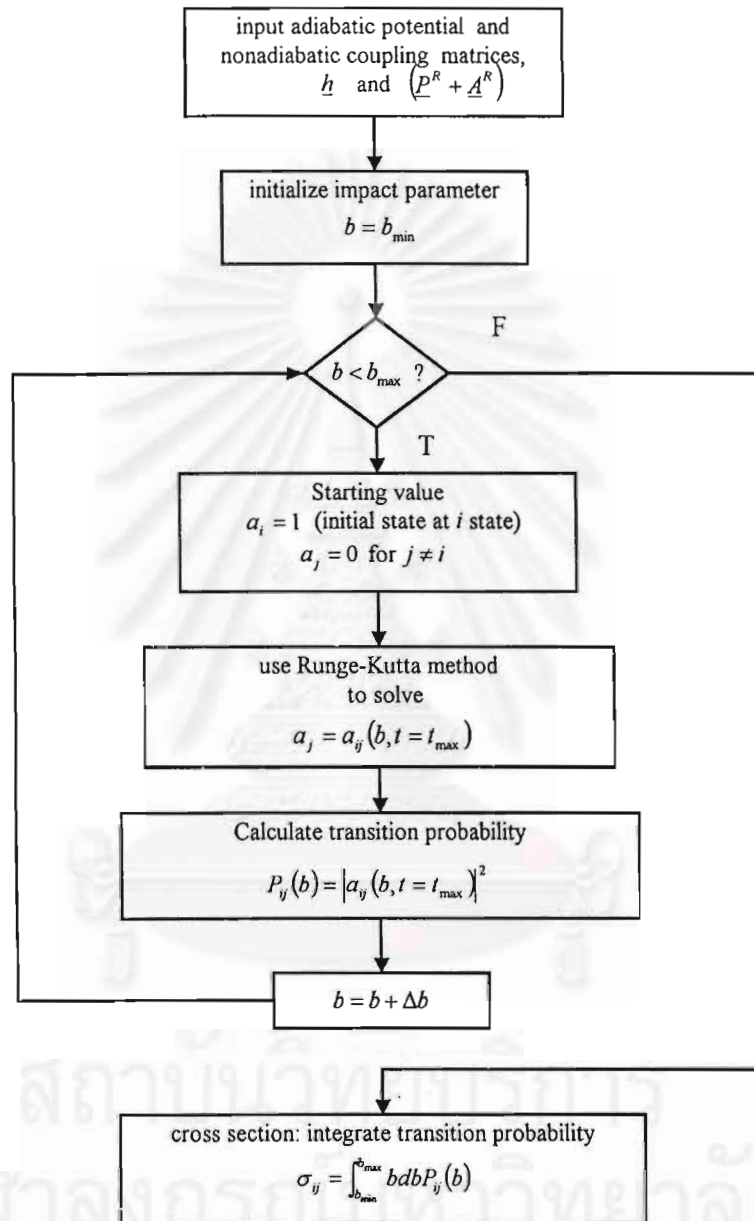


Figure 3.3: Flow chart of the semi-classical calculation procedure.

Chapter 4

The Cross Section and Differential Cross Section of Charge Transfer between O and H^+

The ground state of OH^+ is $X^3\Sigma^-$ [Kimura et al., 1997; Saxon and Liu, 1986; Herzberg, 1950], where $X^3\Sigma^-$ refers to the ground state of the molecular ion (labeled by X), 3 is the spin multiplicity, Σ means that the quantum number m for the angular momentum component along the molecular axis equals zero, and the minus sign implies odd parity along the molecular plane [Herzberg and Spinks, 1950]. In general, the capital Greek letter indicates the value of m : Σ , Π , Δ , etc. refer to $m = 0, 1, 2, \dots$. As shown by Kimura et al. [1997], the OH^+ states

which have important couplings with others during a charge transfer collision are $1^3\Sigma^-$ ($X^3\Sigma^-$), $2^3\Sigma^-$, $3^3\Sigma^-$, $1^1\Pi$, and $2^1\Pi$. These states have configurations and dissociated states as [Saxon and Liu, 1986]

$$\begin{array}{lll}
1^3\Sigma^- & 3\sigma^2 1\pi^2 & \text{O}(^3P) + \text{H}^+ \\
2^3\Sigma^-, 3^3\Sigma^- & 3\sigma 4\sigma 1\pi^2 & \text{O}^+(^4S) + \text{H}(^2S), \text{O}^+(^2D) + \text{H}(^2S) \\
1^1\Pi & 3\sigma 1\pi^3 & \text{O}(^1D) + \text{H}^+ \\
2^1\Pi & 3\sigma^2 4\sigma 1\pi & \text{O}^+(^2D) + \text{H}(^2S).
\end{array}$$

The adiabatic potentials and the coupling matrix elements from Kimura et al. [1997] are shown in Figs. 4.1 and 4.2, respectively. These state configurations were identified by multi-configuration self-consistent field (MCSCF) calculations using the COLUMBUS program [Lischka et al., 1997; Shepard et al., 1988], because Kimura et al. [1997] did not specify the molecular states, or the numerical methods used to find the adiabatic potentials and coupling matrix elements. Kimura et al. [1997] only showed the asymptotic molecular states, which are atomic states. We can identify the molecular state by comparing the results of MCSCF with the results of Kimura et al. [1997]. Those results were only for cross sections in the energy range 0.1-1 keV, but in this thesis we will calculate the cross section and differential cross section in the energy range of 0.8-3.2 keV.

The radial coupling dominates in this process [Kimura et al. 1997], so there are strong transitions only between states of the same angular symmetry. Therefore, we consider three possible transitions: $1^3\Sigma^- \leftrightarrow 2^3\Sigma^-$, $2^3\Sigma^- \leftrightarrow 3^3\Sigma^-$, and $1^1\Pi \leftrightarrow 2^1\Pi$. The angular coupling can be neglected here [Kimura et al.

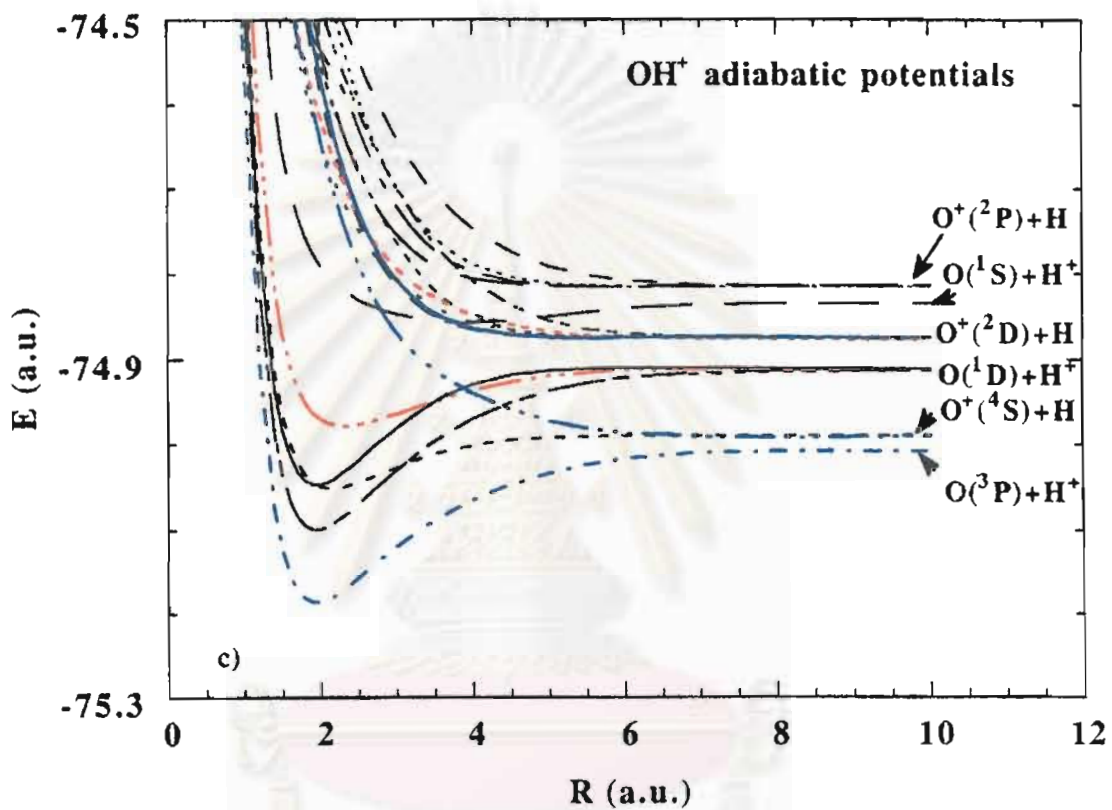


Figure 4.1: Adiabatic potentials of OH⁺ [Kimura et al., 1997]. Blue lines are for ³Σ⁻ states and red lines are for ¹Π states.

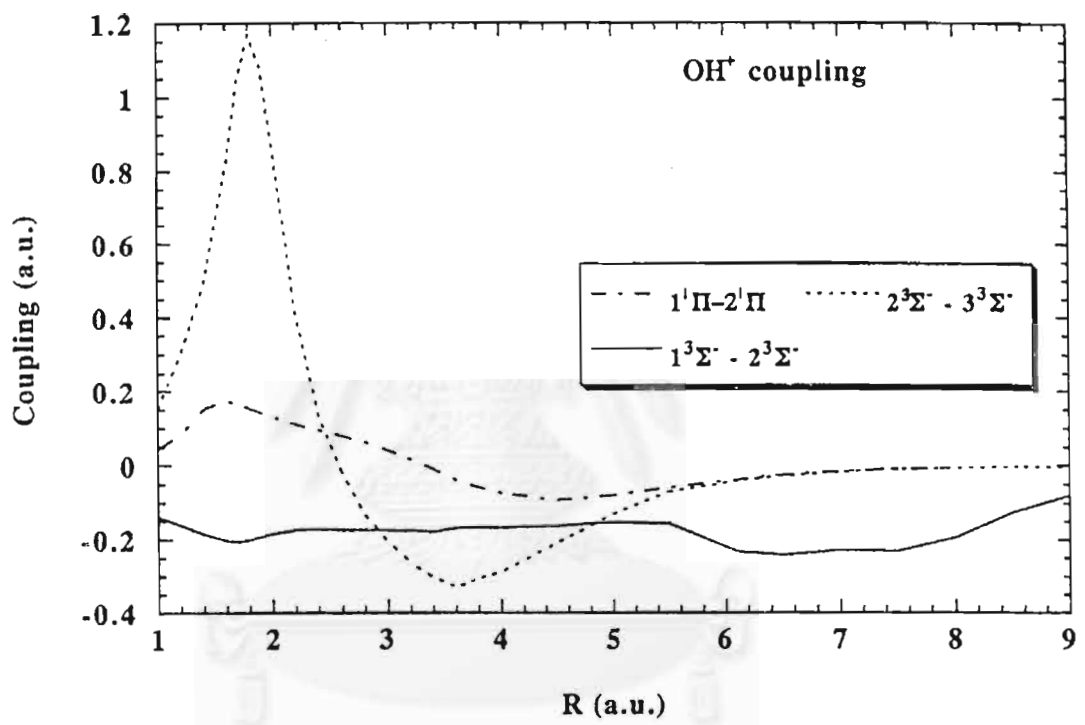


Figure 4.2: Coupling matrix elements [Kimura et al., 1997]

1997], but if there were significant angular coupling, transitions between states of different angular symmetry would occur. The spin-orbit coupling can also be neglected for this energy range. As discussed by Chambaud [1981], the spin-orbit coupling increases when the energy decreases to a few eV. If the spin-orbit coupling is significant, there is coupling between states with different spin multiplicity, implying a possible change of spin multiplicity after collisions. However, at the higher collision energies being considered here, this effect can be neglected. Then there are also no changes of spin multiplicity in the collisions we consider.

4.1 Quantal Calculations

We use the coupling matrix elements and adiabatic potentials from Kimura et al. [1997] to construct the diabatic potentials. In this thesis the starting points of the calculations are at radii lower than the classical turning points. We used the calculation program from R. J. Allen [<http://wserv1.dl.ac.uk/CCP/CCP6/quantx/>]. We have modified the input of the program for using a diabatic potential matrix.

The results for the cross section and differential cross section are shown in Figs. 4.3 to 4.7. For the results of the differential cross section in Figs. 4.3-4.6, there are interference effects as the angle is increased. When the energy increases, the angle of first interference generally decreases.

From equations (B.8) and (B.9) in Appendix B, the formulae for the cross section and differential cross section, in practice we cannot sum the angular

momentum quantum number, l , to infinity, but rather we sum the l to a large value, l_{max} . In the `quantxs` program, there is a limitation in the sum over l in that the maximum value, l_{max} , is not large enough, so the results may have a substantial error. As evidence of this, we have shown that l_{max} actually does affect the calculations of the differential cross section and cross section. When l_{max} was decreased, the cross section and differential cross section decreased. Therefore we should really sum to a very large value of l_{max} , and if the trend continues, this would increase our values for the total and differential cross sections, bringing them into closer agreement with other results.

Figure 4.3 shows the experimental results for the differential cross section [Lindsay et al. 1996]. There are small interference effects between 0.1-1.0 degrees, as most easily seen in the curve for 0.5 keV. For higher energy, there is a larger peak at small angles and a more rapid decrease when increasing the angle, though if we integrate over the scattering angle the total cross sections are of the same order of magnitude. Figure 4.4 shows the only previous theoretical results for the differential cross section [Hedström et al., 1998]. As in the experimental results, there are small interference effects between 0.1-1.0 degrees. These interference effects come from the quantum effects of the scattering. Figure 4.5 shows the present results, and Figure 4.6 shows the comparison of the present results with previous results. These results have values lower than the experimental values, and generally lower than the previous theoretical values, as well as sharper interference effects. We believe that this is because l_{max} in the calculations is not

large enough for convergence of the results. Our results are different than those of Hedström et al., because we use a fully quantal calculation, which is a time-independent problem, but Hedström et al. [1998] used electron nuclear dynamics [Hedström et al., 1998], which is a kind of time-dependent problem, and in the present calculations there was a limit on l_{max} from the program.

Figure 4.7 shows all results for the total cross section, including theoretical results from others [Kimura et al., 1997; Hedström et al., 1998; Hamre et al., 1999], the present results, and experimental results [Stebbing et al., 1964; Lindsay et al., 1996]. The results of the present quantal calculations are again lower than the others, and our quantal results also show an unusual energy dependence. The lower cross section at higher energy may arise because at higher energy, the appropriate value of l_{max} , at which the cross section converges, increases rapidly [Bransden and McDowell, 1992]. In this program there is a limit on l_{max} , which is lower than the appropriate value, and at higher energy we expect greater error. At any rate, our cross sections are still of the same order of magnitude as previous results.

4.2 Semi-classical Calculations

For the semi-classical calculations we used the same coupling matrix elements as in the quantal calculations. We used a straight-line trajectory approximation. A fourth-order Runge-Kutta method was used to solve the coupled time-dependent

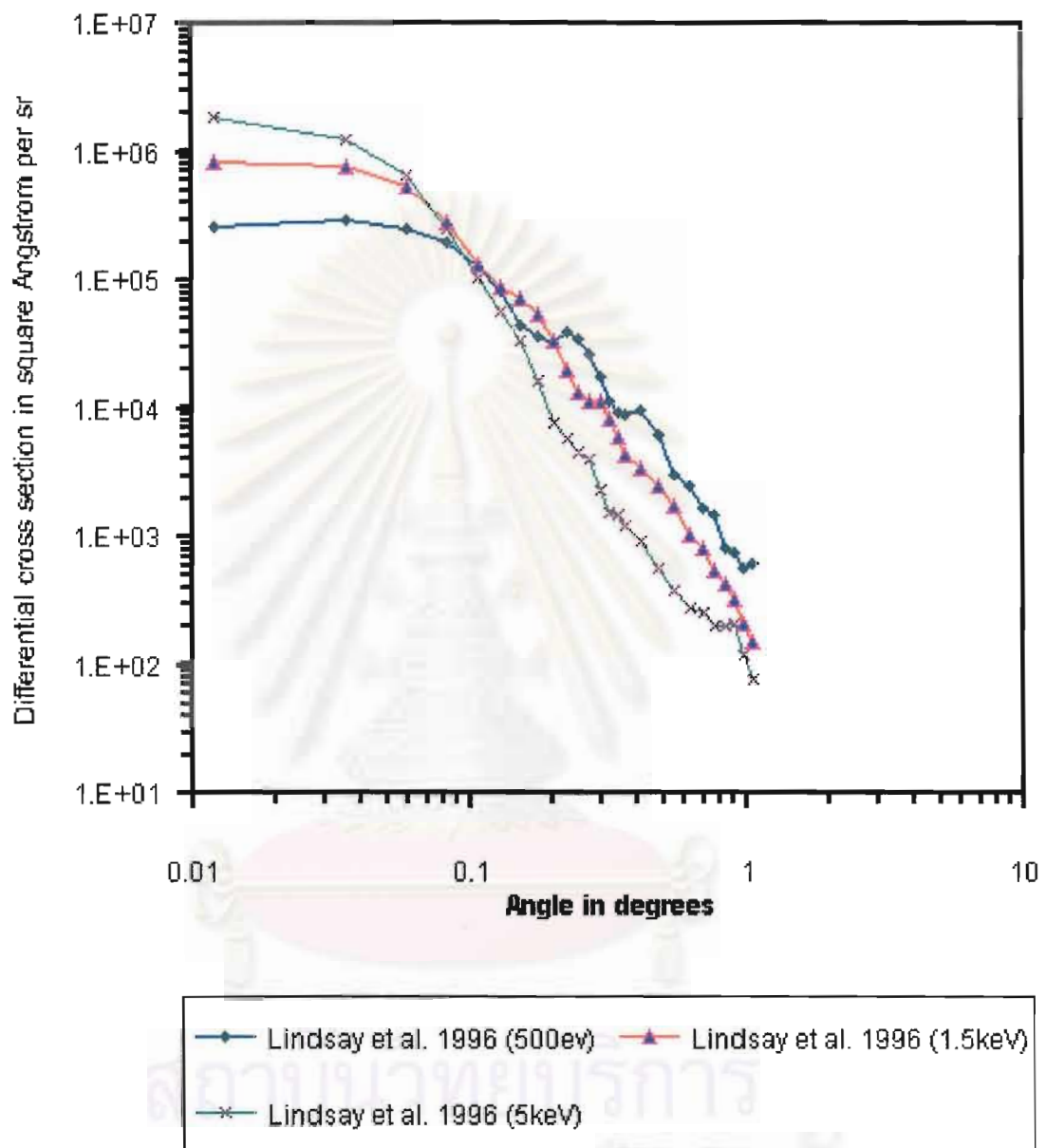


Figure 4.3: The differential cross section for charge transfer: Experimental results [Lindsay et al., 1996]

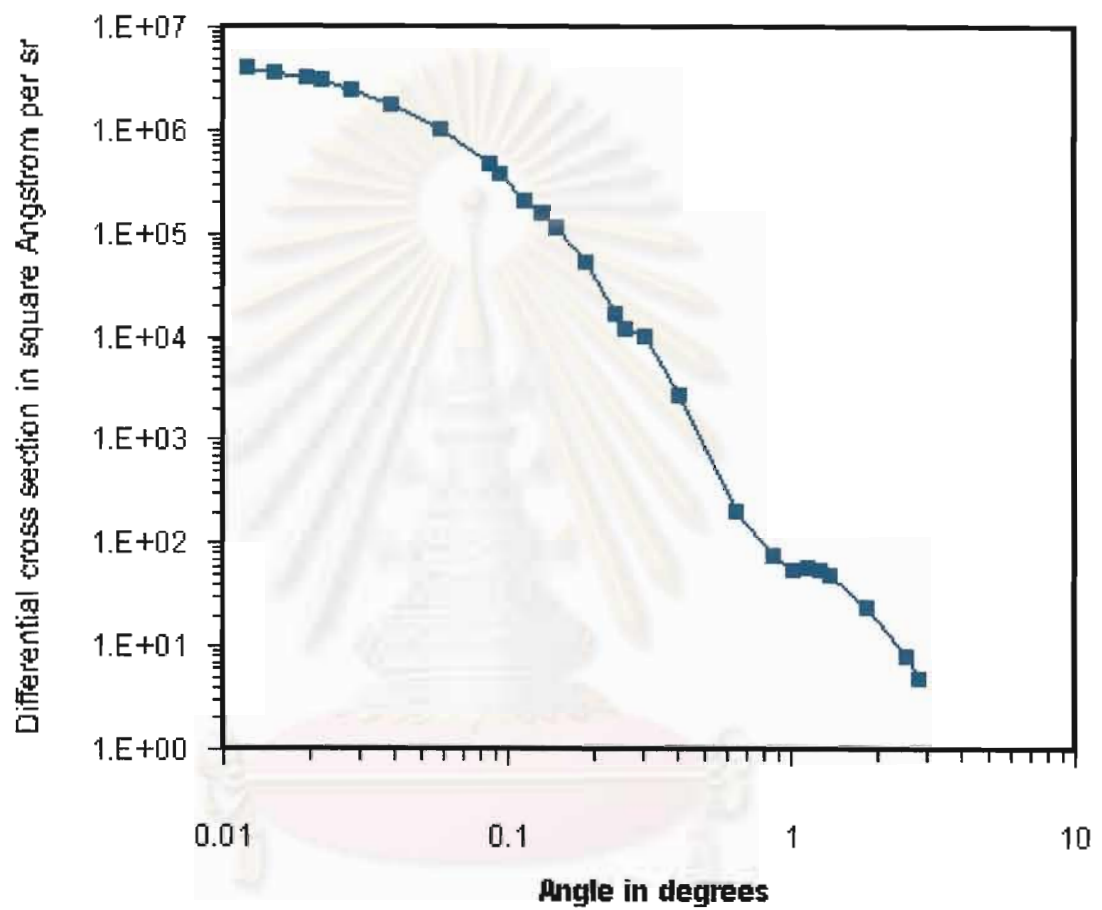


Figure 4.4: The differential cross section for charge transfer: Theoretical results [Hedström et al., 1998]

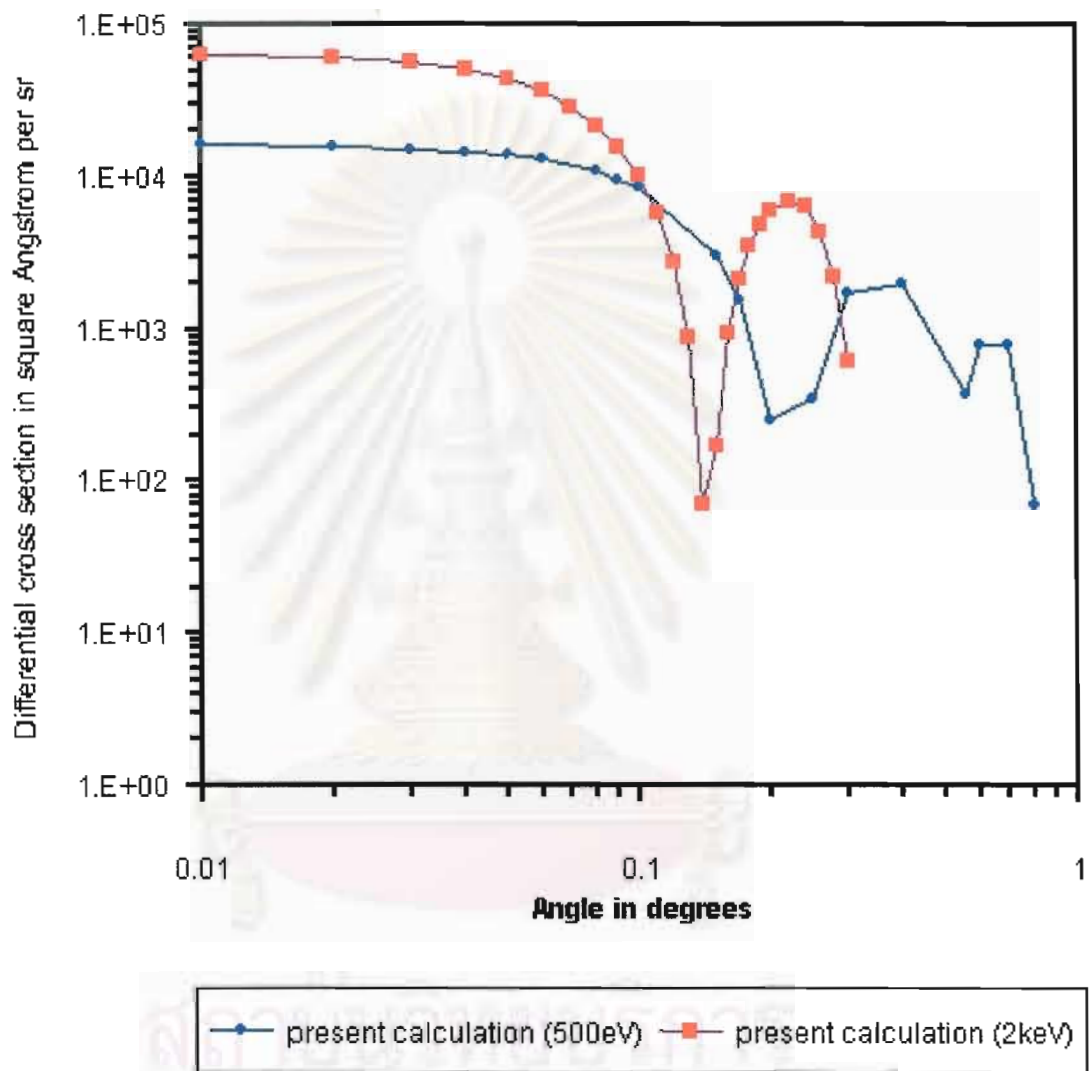


Figure 4.5: The differential cross section for charge transfer: Present calculations

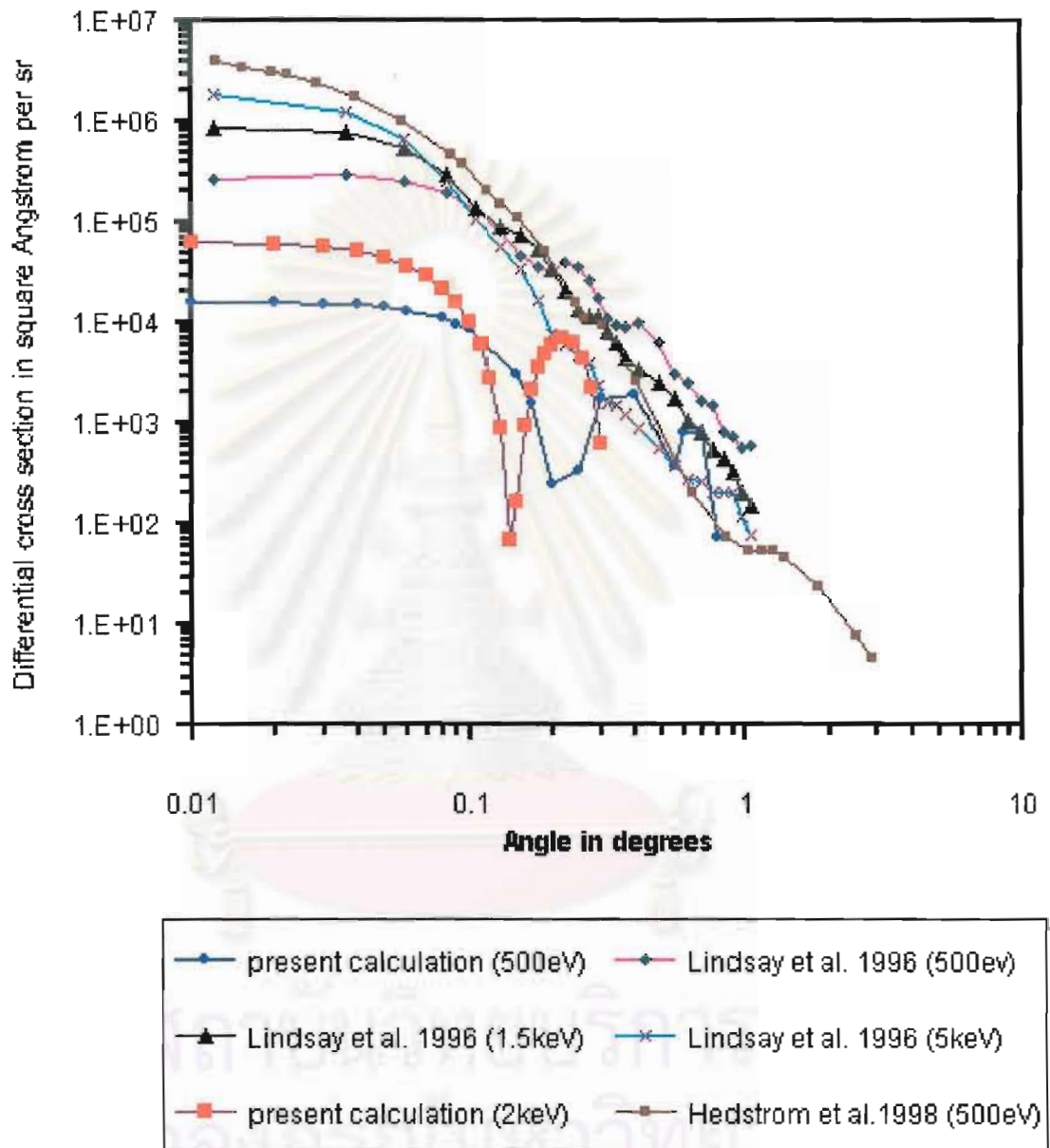


Figure 4.6: The differential cross section for charge transfer: All results

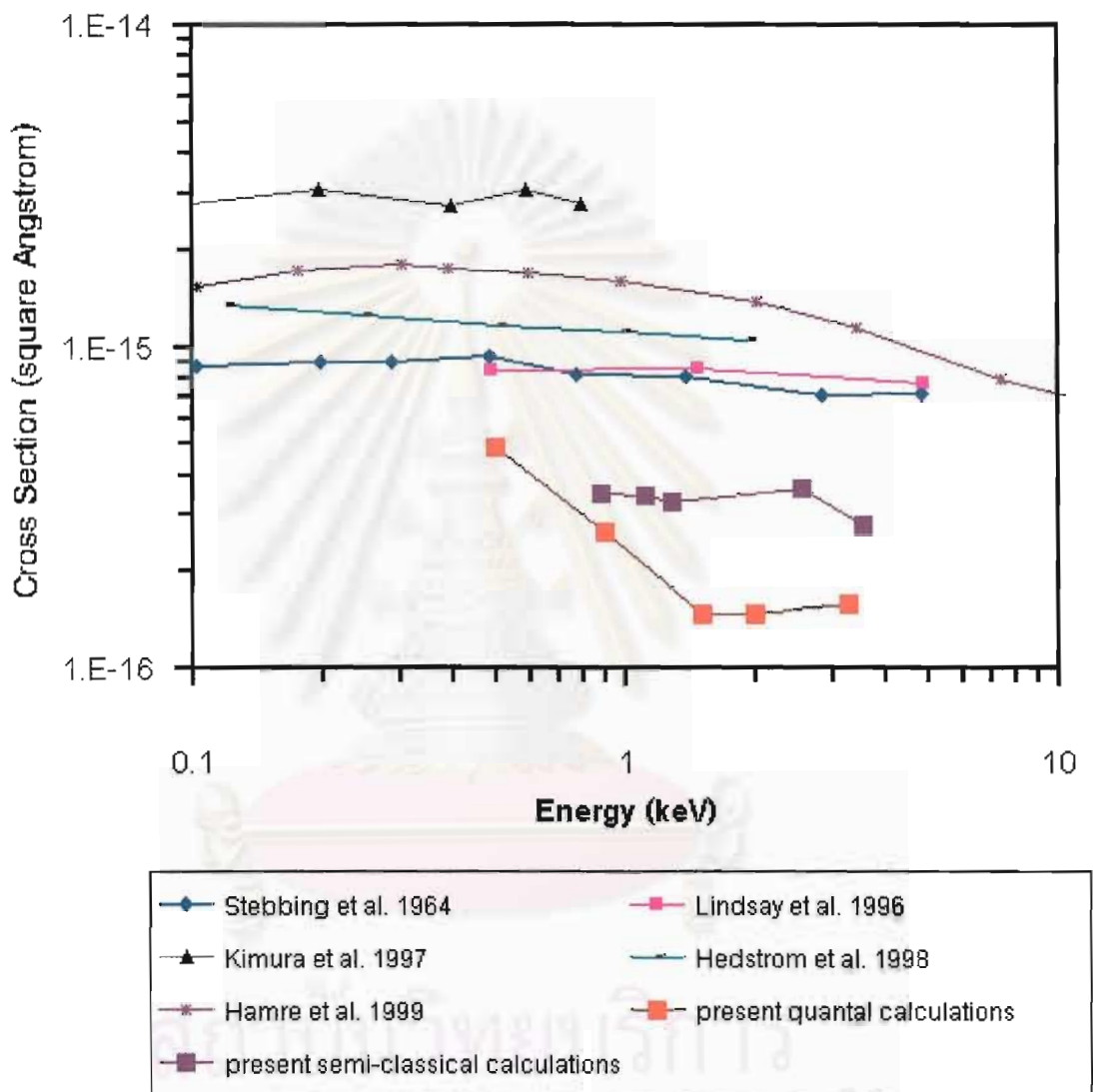
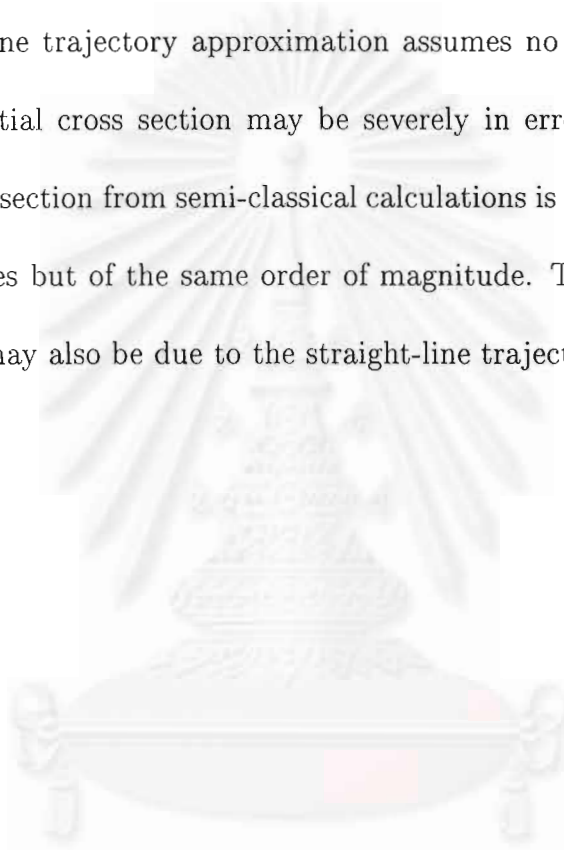


Figure 4.7: The cross section for charge transfer

ODEs, equation (2.47). The result for the cross section is shown in Fig. 4.7. The differential cross sections from the semi-classical calculations poorly match the results of Hedström et al. [1998] and Lindsay et al. [1996]. Our semi-classical results for the differential cross section are lower by about 4 orders of magnitude. The straight-line trajectory approximation assumes no deflection of the nuclei, so the differential cross section may be severely in error. On the other hand, the total cross section from semi-classical calculations is smaller than values from previous studies but of the same order of magnitude. These lower values of the cross section may also be due to the straight-line trajectory approximation.



สถาบันวิทยบริการ
จุฬาลงกรณ์มหาวิทยาลัย

Chapter 5

Conclusions

The charge exchange of O and H^+ is of interest to many people. Many people have calculated the total cross section for a range of collision energies, but there has been little research about differential cross sections. The differential cross section was calculated only at the energy of 0.5 keV [Hedström et al., 1998], and experimental results are available only for 0.5, 1.5, and 5.0 keV. In this thesis, the differential cross section and cross section were calculated by quantal calculations at energies of 0.5 keV, 1.0 keV, 2 keV, and 3.5 keV, because this energy range corresponds to solar wind speeds, i.e., the collision speeds expected near the solar wind termination shock.

In the last chapter, the results from approximate semi-classical calculations are acceptable only in terms of the total cross section. The differential cross section is lower by four orders of magnitude compared with other calculations and experimental data. Essentially, the angular region of scattering is far too

narrow in these approximate semi-classical calculations. We suggest that this discrepancy may result from the straight-line approximation (i.e., that both nuclei travel along straight lines during the collision), which is used because in the semi-classical formulation we do not know the interaction between the ion and atom in order to construct the trajectory.

For the quantal calculations, the differential cross section was compared with those calculated by Hedström et al. [1998] and the experiment of Lindsay et al. [1996]. The cross section was compared with the theoretical results of Kimura et al. [1997], Hedström et al. [1998], and Hamre et al. [1999], and the experimental results of Stebbings et al. [1964] and Lindsay et al. [1996]. Both types of results in this thesis are lower, but not drastically different from other results given the spread among the previous results themselves. In this calculation, the number of angular momentum values in the partial wave expansion (see Appendix B) was limited by the numerical algorithm. Therefore, this calculation can be further improved by increasing the number of angular momentum values considered in the expansion.

สถาบันวิทยบริการ
จุฬาลงกรณ์มหาวิทยาลัย

References

- Bransden, B. H. and McDowell, M. R. C. 1992. **Charge Exchange and the Theory of Ion-Atom Collisions**. New York: Oxford.
- Chambaud, G., Launay, J. M., Levy, B., Millie, P., Roueff, E. and Minh, F. T. 1980. "Charge Exchange and Fine-Structure Excitation in O-H⁺ Collisions." **J. Phys. B** 13: 4205-4216.
- Child, M. S. 1974. **Molecular Collision Theory**. London: Academic Press.
- Delos, J. B. 1981. "Theory of Electronic Transitions in Slow Atomic Collisions." **Rev. Mod. Phys.** 53: 287-357.
- Errea, K. F., Mendez, L. and Riera, A. 1982. **J. Phys. B** 15: 101.
- Field, G. B. and Steigman, G. 1971. "Charge Transfer and Ionization Equilibrium in the Interstellar Medium." **Astrophys. J.** 166: 59-64.
- Gordon, R. G. 1969. "New Method for Constructing Wavefunctions for Bound States and Scattering." **J. Chem. Phys.** 51: 14-25.
- Hamre, B., Hansen, J. P. and Kocbach, L. 1999. "Cross Section for Capture,

- Excitation and Ionization in Proton-Oxygen Collisions.” **J. Phys. B** 32: L127-L131.
- Hedström, M., Deumens, E., and Öhrn, Y. 1998. “Electron Nuclear Dynamics of Charge-Transfer Collisions of Protons with Atomic Oxygen.” **Phys. Rev. A** 57: 2625-2628.
- Herzberg, G. and Spinks, J. W. T. 1950. **Molecular Spectra and Molecular Structure, I. Spectra of Diatomic Molecules**. Toronto: D. Van Nostrand Company.
- Janev, R. K., Winter, H. P. and Fritsch, W. 1995. “Electron Capture Processes in Slow Collisions of Plasma Impurity Ions with H, H₂ and He” In R. K. Janev (ed.), **Atomic and Molecular Processes in Fusion Edge Plasmas** New York: Plenum.
- Johnson, B. R. 1973. “The Multichannel Log-Derivative Method for Scattering Calculations.” **J. Comput. Phys.** 13: 445-449.
- Kimura, M., Gu, J. P., Hirsch, G. and Guenker, R. J. 1997. “Inelastic Processes in Collisions of H⁺ Ions with C, N, O, and Si Atoms below 1 keV.” **Phys. Rev. A** 55: 2778-2785.
- Kimura, M. and Lane, N. F. 1989. “The Low-Energy Heavy-Particle Collisions—A Close-Coupling Treatment.” In D. R. Bates and B. Bederson (eds.), **Advances in Atomic and Molecular Optical Physics**, Vol. 26, pp. 79-160. New York: Academic Press.

- Lebeda, C. F. and Thorson, W. R. 1971. "Impact Ionization in the Proton-H-Atom System. IV. Improved Values for Radial Transition Matrix Elements." **Phys. Rev.** 4: 900-907.
- Lee, M. A. 1996. "The Termination Shock of the Solar Wind." **Space Science Reviews** 78: 109-116.
- Levy, H. H. and Thorson, W. R. 1969. **Phys. Rev.** 181: 252.
- Lindsay, B. G., Sieglaff, D. R., Schafer, D. A., Hakes, C. L., Smith, K. A. and Stebbings, R. F. 1996. "Charge Transfer of 0.5-, 1.5-, and 5-keV Protons with Atomic Oxygen: Absolute Differential and Integral Cross Sections." **Phys. Rev. A** 53: 212-218.
- Lischka, H., Shepard, R., Shavitt, I., Brown, F. B., Pitzer, R. M., Ahlrichs, R., Böhm H, J., Chang, A. H. H., Comeau, R., Gdanitz, R., Dachsel, H., Dallos, M., Erhard, C., Ernzerhof, M., Gawboy, G., Höchtel, P., Irle, S., Kedziora, G., Kovar, T., Müller, Th., Parasuk, V., Pepper, M., Scharf, P., Schiffer, H., Schindler, M., Schüler, M., Stahlberg, E., Szalay, P. G. and Zhao, J. G. 1997. "COLUMBUS: An *ab initio* Electronic Structure Program, Release 5.3."
- Manolopoulos, D. E. 1986. "An Improved Log Derivative Method for Inelastic Scattering." **J Chem. Phys.** 85: 6425-6429.
- Messiah, A. 1970. **Quantum Mechanics**, Amsterdam: North-Holland.
- Michelis, P. D. and Orsini, S. 1997. "Energetic Neutral Atoms Propagating toward the Earth: Analysis of the Reduction Rate due to Ionospheric and

- Atmospheric Interactions.” **J. Geophys. Res.** 102: 185-193.
- Mittleman, M. H. and Tai, H. 1973. **Phys. Rev. A** 8: 1880.
- Péquiugnot, D. 1990. “Populations of the O I Metastable Levels.” **Astron. Astrophys.** 231: 499-508.
- Picone, J. M., Meier, R. R., Kelly, O. A., Dymond, K. F., Thomas, R. J., Melendez-Alvira, D. J. and McCoy, R. P. 1997. “Investigation of Ionospheric O⁺ Remote Sensing Using the 834-Å Airglow.” **J. Geophys. Res.** 102: 2441-2456.
- Saxon, R. P. and Liu, B. 1986. “Theoretical Study of OH⁺: Potential Curves, Transition Moment, and Photodissociation Cross Section.” **J. Chem. Phys.** 85: 2099-2104.
- Schunk, R. W. and Nagy, A. F. 1980. “Ionospheres of the Terrestrial Planets.” **Rew. Geophys. Space Phys.** 18: 813-852.
- Schneiderman, S. B., and Russek, A. 1969. “Velocity-Dependent Orbitals in Proton-On-Hydrogen-Atom Collisions.” **Phys. Rev.** 181: 311-321.
- Shepard, R., Shavitt, I, Pitzer, R. M., Comeau, D. C., Pepper, M., Lischka, H., Szalay, P. G., Ahlrichs, R., Brown, F. B., and Zhao, J. G. 1988. **Int. J. Quantum Chem.** S22: 149.
- Spjeldvik, W. N. and Fritz, T. A. 1978. “Theory for Charge States of Energetic Oxygen Ions in the Earth’s Radiation Belts.” **J. Geophys. Res.** 83: 1583-1594.

- Spjeldvik, W. N. 1979. "Expected Charge States of Energetic Ions in the Magnetosphere." 23: 499-538.
- Stebbing, R. F., Smith, A. C. H. and Ehrhardt, H. 1964. "Charge Transfer between Oxygen Atoms and O^+ and H^+ Ions." **J. Geophys. Res.** 69: 2349-2355.
- Stone, E. C., Cummings, A. C. and Webber, W. R. 1996. "The Distance to the Solar Wind Termination Shock in 1993 and 1994 from Observations of Anomalous Cosmic Rays." **J. Geophys. Res.** 101: 11017-11025.
- Thorson, W. R. and Delos, J. B. 1978. "Theory of Near-Adiabatic Collisions. I. Electron Translation Factor Methods." **Phys. Rev. A** 18: 117-134.
- Thorson, W. R. and Delos, J. B. 1978. "Theory of Near-Adiabatic Collisions. II. Scattering Coordinate Method." **Phys. Rev. A** 18: 135-155.
- Vaaben, J. and Taulbjerg, K. 1986. **J. Phys. B** 14: 1815.

สถาบันวิทยบริการ
จุฬาลงกรณ์มหาวิทยาลัย

Appendix A

Various Forms of Switching Functions

[from Kimura and Lane 1989]

1. By Schneiderman and Russek [1969]:

$$\frac{\cos(\theta)}{1 + (\alpha/R)^2} \quad (\text{A.1})$$

θ : angle between electron motion and internuclear separation of
projectile and target

α : state-independent parameter

2. By Levy and Thorson [1969] (cited by Kimura et al. [1989]):

$$\frac{r_B^2 - r_A^2}{r_B^2 + r_A^2} \quad (\text{A.2})$$

3. By Lebeda et al. [1971]:

$$\tanh(R\beta_n\eta) \quad (\text{A.3})$$

$$\eta = (r_B - r_A)/R$$

β_n : state-dependent parameter

4. By Mittleman and Tai [1973] (cited by Kimura et al. [1989]):

$$\frac{(1 - S^2)(1 - e^{-2\alpha\eta})}{(1 + S^2)(1 + e^{-2\alpha\eta}) - 4Se^{-\alpha\eta}} \quad (\text{A.4})$$

S: overlap of LCAO

α : Slater exponent

$$\eta = |\vec{r} + \frac{1}{2}\vec{R}| - |\vec{r} - \frac{1}{2}\vec{R}|$$

5. By Rankin and Thorson [1979] (cited by Kimura et al. [1989]):

$$\tanh R \left\{ \frac{1}{2} \beta_n [(Z_B + Z_A) + (Z_B - Z_A)] + \alpha_n \ln \frac{Z_A}{Z_B} \right\} \quad (\text{A.5})$$

α_n : state-dependent parameter

6. By Vaaben and Taulbjerg [1981] (cited by Kimura et al. [1989]):

$$\frac{1}{2} \left(\frac{Z_A r_B^3 - Z_B r_A^3}{Z_A r_B^3 + Z_B r_A^3} + \frac{Z_A - Z_B}{Z_A + Z_B} \right) \quad (\text{A.6})$$

7. By Errea et al. [1982] (cited by Kimura et al. [1989]):

$$\frac{R^2}{R^2 + \beta^2} \frac{\tilde{Z}}{R + \alpha} \quad (\text{A.7})$$

\tilde{Z} : Z-coordinate of electron position

α, β : state-independent parameter

The state-dependent parameters can be found by optimizing the coupling matrix according to the variation method of quantum mechanics.

Appendix B

Partial Wave Expansion

[from Child 1974]

Starting with the Schödinger equation,

$$[\nabla_R^2 + k_i^2] \Psi_i(\vec{R}) = \sum_j U_{ij}(\vec{R}) \Psi_j(R) \quad (\text{B.1})$$

If the potential is spherically symmetric, $V(\vec{R}) = V(R)$; hence the orbital and rotational angular momenta are both constants of the motion.

We can expand the wave function as

$$\Psi_j(\vec{R}) = \frac{1}{R} \sum_{l=0}^{\infty} A_l \psi(R) P_l(\cos \theta), \quad (\text{B.2})$$

where P_l is the Legendre polynomial of order l . This leads to equations for the radial function $\psi_{jl}(R)$,

$$\left[\frac{d^2}{dR^2} + k_i^2 - \frac{l(l+1)}{R^2} \right] \psi_{il}(R) = \sum_j U_{ij}(R) \psi_{jl}(R). \quad (\text{B.3})$$

Each orbital angular momentum quantum number l therefore gives rise to a different set of coupled equations and a different S matrix, $\underline{S}^{(l)}$. The asymptotic

solution is

$$\begin{aligned}\psi_{il}^{(i)}(R) &\sim \sin\left(k_i R - \frac{l\pi}{2}\right) - \frac{1}{2}T_{ii}^{(l)}e^{ik_i R - il\pi/2} \\ \psi_{jl}^{(i)}(R) &\sim -\frac{1}{2}\left(\frac{k_i}{k_j}\right)^{\frac{1}{2}}T_{ij}^{(l)}e^{ik_j R - il\pi/2},\end{aligned}\quad (\text{B.4})$$

and the choice of the coefficient in equation (B.3), now labelled $A_l^{(i)}$, is such that the incoming part of $\Psi_i(\vec{R})$ behaves as the incoming part of a plane wave.

Equation (B.3) requires the asymptotic form

$$\Psi_j(R) = \delta_{ij}e^{ik_j z} + \frac{f_{ij}(\theta)e^{ik_j R}}{R}, \quad (\text{B.5})$$

where

$$\begin{aligned}f_{ij}(\theta) &= -\frac{1}{2[k_i k_j]^{\frac{1}{2}}}\sum_{l=0}^{\infty}(2l+1)T_{ij}^{(l)}P_l(\cos\theta) \\ &= -\frac{1}{2[k_i k_j]^{\frac{1}{2}}}\sum_{l=0}^{\infty}(2l+1)(S_{ij}^{(l)} - \delta_{ij})P_l(\cos\theta)\end{aligned}\quad (\text{B.6})$$

and the transition matrix, \underline{T} and scattering matrix, \underline{S} are related by

$$T_{ij} = \delta_{ij} - S_{ij}. \quad (\text{B.7})$$

The differential cross section is dependent on the square of scattering amplitude,

$$\begin{aligned}\frac{d\sigma_{ij}}{d\Omega} &= \frac{k_j}{k_i}|f_{ij}(\theta)|^2 \\ &= \frac{1}{4k_i^2}\left|\sum_{l=0}^{\infty}(2l+1)T_{ij}^{(l)}P_l(\cos\theta)\right|^2\end{aligned}\quad (\text{B.8})$$

and the cross section is

$$\begin{aligned}\sigma_{ij} &= \frac{k_j}{k_i}\int_0^{2\pi}\int_0^\pi|f_{ij}(\theta)|^2\sin\theta d\theta d\phi \\ &= \frac{\pi}{k_i^2}\sum_{l=0}^{\infty}(2l+1)|T_{ij}^{(l)}|^2.\end{aligned}\quad (\text{B.9})$$

Appendix C

Program for Semi-classical Calculations

This program was written by Suphachai Aukaraputporn, as supervised and modified by Saree Phongphananee. Paisan Tooprakai also helped with debugging.

A flow chart of this program is presented in Figure 3.3.

```
#include <stdio.h>
#include <math.h>
double H=0.001;
double diff_x1(double vr,double paa12,double h1,double x2,double y1,double y2,
double w12)
{
return h1*y1 + vr*paa12*(-y2*cos(w12)+x2*sin(w12));
}
double diff_x2(double vr,double paa12,double paa23,double h2,double x1,
double x3,double y1,double y2,double y3,double w21,double w23)
{
return h2*y2 + vr*paa12*(-y1*cos(w21)+x1*sin(w21))
+ vr*paa23*(-y3*cos(w23)+x3*sin(w23)) ;
}
double diff_x3(double vr,double paa23,double h3,double x2,double y2,double y3,
double w32)
{
return h3*y3 + vr*paa23*(-y2*cos(w32)+x2*sin(w32)) ;
}
double diff_y1(double vr,double paa12,double h1,double x1,double x2,double y2,
double w12)
{
return -h1*x1 + vr*paa12*(x2*cos(w12)+y2*sin(w12));
}
```

```

double diff_y2(double vr,double paa12,double paa23,double h2,double x1,
double x2,double x3,double y1,double y3,double w21,double w23)
{
return -h2*x2 + vr*paa12*(x1*cos(w21)+y1*sin(w21))
+ vr*paa23*(x3*cos(w23)+y3*sin(w23));
}
double diff_y3(double vr,double paa23,double h3,double x2,double x3,double y2,
double w32)
{
return -h3*x3 + vr*paa23*(x2*cos(w32)+y2*sin(w32)) ;
}
void cubic_splines(double z[],double Bx[],double d2x[],int n)
{
int i,j,k,N;
double A[100][100],bx[100],koon,beta[100],rho[100];
N = n-1;
for(i=1;i<=N-1;i++){
A[i][i] = 2.0*(z[i+1]-z[i-1]);
A[i][i+1] = z[i+1]-z[i];
A[i][i-1] = z[i]-z[i-1];
bx[i] = 6.0*((Bx[i+1]-Bx[i])/(z[i+1]-z[i])
-(Bx[i]-Bx[i-1])/(z[i]-z[i-1]));
}
for(i=2;i<=N-1;i++){
koon = -A[i][i-1]/A[i-1][i-1];
A[i][i] += koon*A[i-1][i];
bx[i] += koon*bx[i-1];
}
d2x[N-1]=bx[N-1]/A[N-1][N-1];
for(i=N-2;i>=1;i--){
d2x[i] = (bx[i]-A[i][i+1]*d2x[i+1])/A[i][i];
}
d2x[0] = 0.0;
d2x[N] = 0.0;
}
double interpolate(double z,int n,double Z[],double B[],double d2[])
{
int i,N;
double D1,D2,DD,T1,T2,T3,T4,Mag;
z=fabs(z);
N=n-1;
if( z<Z[0] || z>Z[N] ){
printf("\nThere are not enough data");
exit(1);
}
for(i=0;i<=N-1;i++){
if((z > Z[i] && z < Z[i+1]) || z == Z[i] || z == Z[i+1]) {
D1 = Z[i+1]-z;
D2 = z-Z[i];
DD = Z[i+1]-Z[i];
T1 = ( d2[i]*D1*D1*D1 ) / ( 6.0*DD );
T2 = ( d2[i+1]*D2*D2*D2 ) / ( 6.0*DD );
T3 = ( (B[i+1]/DD) - (d2[i+1]*DD/6.0) ) * D2;
T4 = ( (B[i]/DD) - (d2[i]*DD/6.0) ) * D1;
Mag = T1+T2+T3+T4;
}
}
return Mag;
}
double omega(double h1old,double h2old,double h1,double h2,double w12)
{
return w12+(h2-h1+h2old-h1old)*H/4.0;
}
double Runge_kutta(double r,double b,double v,double t,double *x1,double *y1,
double *x2,double *y2,double *x3,double *y3,double r_pa12[],

```

```

double pa12[],double d2_pa12[],double r_pa23[],double pa23[],
double d2_pa23[],double r_h1[],double hh1[],double d2_h1[],
double r_h2[],double hh2[],double d2_h2[],double r_h3[],double hh3[],
double d2_h3[],int n_pa12,int n_pa23,int n_h1,int n_h2,int n_h3)
{
int i,n;
double limit,vr,paa12,paa23,h1,h2,h3,w12,w21,w23,w32,tt;
double kx1_1,kx1_2,kx1_3,kx1_4,
      kx2_1,kx2_2,kx2_3,kx2_4,
      kx3_1,kx3_2,kx3_3,kx3_4;
double ky1_1,ky1_2,ky1_3,ky1_4,
      ky2_1,ky2_2,ky2_3,ky2_4,
      ky3_1,ky3_2,ky3_3,ky3_4;
double h1old,h2old,h3old;
limit=-t;
w12=0.0;
w23=0.0;
if(t<=0)
vr = v*cos(asin(b/r));
else
vr = -v*cos(asin(b/r));
paa12=interpolate(r,n_pa12,r_pa12,pa12,d2_pa12);
paa23=interpolate(r,n_pa23,r_pa23,pa23,d2_pa23);
h1=h1old=interpolate(r,n_h1,r_h1,hh1,d2_h1);
h2=h2old=interpolate(r,n_h2,r_h2,hh2,d2_h2);
h3=h3old=interpolate(r,n_h3,r_h3,hh3,d2_h3);
w12=omega(h1old,h2old,h1,h2,w12);
w21=-w12;
w23=omega(h2old,h3old,h2,h3,w23);
w32=-w23;
do{
kx1_1=diff_x1(vr,paa12,h1,*x2,*y1,*y2,w12);
kx2_1=diff_x2(vr,paa12,paa23,h2,*x1,*x3,*y1,*y2,*y3,w21,w23);
kx3_1=diff_x3(vr,paa23,h3,*x2,*y2,*y3,w32);
ky1_1=diff_y1(vr,paa12,h1,*x1,*x2,*y2,w12);
ky2_1=diff_y2(vr,paa12,paa23,h2,*x1,*x2,*x3,*y1,*y3,w21,w23);
ky3_1=diff_y3(vr,paa23,h3,*x2,*x3,*y2,w32);
tt=t+H/2.0;
r=sqrt((b*b)+((v*v)*(tt*tt)));
if(t<=0)
vr = v*cos(asin(b/r));
else
vr = -v*cos(asin(b/r));
paa12=interpolate(r,n_pa12,r_pa12,pa12,d2_pa12);
paa23=interpolate(r,n_pa23,r_pa23,pa23,d2_pa23);
h1=interpolate(r,n_h1,r_h1,hh1,d2_h1);
h2=interpolate(r,n_h2,r_h2,hh2,d2_h2);
h3=interpolate(r,n_h3,r_h3,hh3,d2_h3);
w12=omega(h1old,h2old,h1,h2,w12);
w21=-w12;
w23=omega(h2old,h3old,h2,h3,w23);
w32=-w23;
h1old=h1;
h2old=h2;
h3old=h3;
kx1_2=diff_x1(vr,paa12,h1,*x2+(kx2_1*H/2.0),*y1+(ky1_1*H/2.0),
      *y2+(ky2_1*H/2.0),w12);
kx2_2=diff_x2(vr,paa12,paa23,h2,*x1+(kx1_1*H/2.0),*x3+(kx3_1*H/2.0),
      *y1+(ky1_1*H/2.0),*y2+(ky2_1*H/2.0),*y3+(ky3_1*H/2.0),w21,w23);
kx3_2=diff_x3(vr,paa23,h3,*x2+(kx2_1*H/2.0),*y2+(ky2_1*H/2.0),
      *y3+(ky3_1*H/2.0),w32);
ky1_2=diff_y1(vr,paa12,h1,*x1+(kx1_1*H/2.0),*x2+(kx2_1*H/2.0),
      *y2+(ky2_1*H/2.0),w12);
ky2_2=diff_y2(vr,paa12,paa23,h2,*x1+(kx1_1*H/2.0),*x2+(kx2_1*H/2.0),
      *x3+(kx3_1*H/2.0),*y1+(ky1_1*H/2.0),*y3+(ky3_1*H/2.0),w21,w23);

```

```

ky3_2=diff_y3(vr,paa23,h3,*x2+(kx2_1*H/2.0),*x3+(kx3_1*H/2.0),
*y2+(ky2_1*H/2.0),w32);
kx1_3=diff_x1(vr,paa12,h1,*x2+(kx2_2*H/2.0),*y1+(ky1_2*H/2.0),
*y2+(ky2_2*H/2.0),w12);
kx2_3=diff_x2(vr,paa12,paa23,h2,*x1+(kx1_2*H/2.0),*x3+(kx3_2*H/2.0),
*y1+(ky1_2*H/2.0),*y2+(ky2_2*H/2.0),*y3+(ky3_2*H/2.0),w21,w23);
kx3_3=diff_x3(vr,paa23,h3,*x2+(kx2_2*H/2.0),*y2+(ky2_2*H/2.0),
*y3+(ky3_2*H/2.0),w32);
ky1_3=diff_y1(vr,paa12,h1,*x1+(kx1_2*H/2.0),*x2+(kx2_2*H/2.0),
*y2+(ky2_2*H/2.0),w12);
ky2_3=diff_y2(vr,paa12,paa23,h2,*x1+(kx1_2*H/2.0),*x2+(kx2_2*H/2.0),
*x3+(kx3_2*H/2.0),*y1+(ky1_2*H/2.0),*y3+(ky3_2*H/2.0),w21,w23);
ky3_3=diff_y3(vr,paa23,h3,*x2+(kx2_2*H/2.0),*x3+(kx3_2*H/2.0),
*y2+(ky2_2*H/2.0),w32);
tt=t+H;
r=sqrt(b*b + v*v*tt*tt);
if(t<=0)
vr = v*cos(asin(b/r));
else
vr = -v*cos(asin(b/r));
paa12=interpolate(r,n_pa12,r_pa12,pa12,d2_pa12);
paa23=interpolate(r,n_pa23,r_pa23,pa23,d2_pa23);
h1=interpolate(r,n_h1,r_h1,hh1,d2_h1);
h2=interpolate(r,n_h2,r_h2,hh2,d2_h2);
h3=interpolate(r,n_h3,r_h3,hh3,d2_h3);
w12=omega(h1old,h2old,h1,h2,w12);
w21=-w12;
w23=omega(h2old,h3old,h2,h3,w23);
w32=-w23;
h1old=h1;
h2old=h2;
h3old=h3;
kx1_4=diff_x1(vr,paa12,h1,*x2+(kx2_3*H),*y1+(ky1_3*H),
*y2+(ky2_3*H),w12);
kx2_4=diff_x2(vr,paa12,paa23,h2,*x1+(kx1_3*H),*x3+(kx3_3*H),
*y1+(ky1_3*H),*y2+(ky2_3*H),*y3+(ky3_3*H),w21,w23);
kx3_4=diff_x3(vr,paa23,h3,*x2+(kx2_3*H),*y2+(ky2_3*H),
*y3+(ky3_3*H),w32);
ky1_4=diff_y1(vr,paa12,h1,*x1+(kx1_3*H),*x2+(kx2_3*H),
*y2+(ky2_3*H),w12);
ky2_4=diff_y2(vr,paa12,paa23,h2,*x1+(kx1_3*H),*x2+(kx2_3*H),
*x3+(kx3_3*H),*y1+(ky1_3*H),*y3+(ky3_3*H),w21,w23);
ky3_4=diff_y3(vr,paa23,h3,*x2+(kx2_3*H),*x3+(kx3_3*H),
*y2+(ky2_3*H),w32);
*x1+=(kx1_1+2.0*kx1_2+2.0*kx1_3+kx1_4)*(H/6.0);
*x2+=(kx2_1+2.0*kx2_2+2.0*kx2_3+kx2_4)*(H/6.0);
*x3+=(kx3_1+2.0*kx3_2+2.0*kx3_3+kx3_4)*(H/6.0);
*y1+=(ky1_1+2.0*ky1_2+2.0*ky1_3+ky1_4)*(H/6.0);
*y2+=(ky2_1+2.0*ky2_2+2.0*ky2_3+ky2_4)*(H/6.0);
*y3+=(ky3_1+2.0*ky3_2+2.0*ky3_3+ky3_4)*(H/6.0);
/* printf("%lf %lf %lf %lf %lf \n",*x1**x1+*y1**y1,*x2**x2+*y2**y2,
*x3**x3+*y3**y3,*x1**x1+*y1**y1+*x2**x2+*y2**y2+*x3**x3+*y3**y3,r);
*/ t+=H;
} while(t<limit);
return 0;
}

void read(double R[],double V[],int *N,char name[])
{
    int i;
    FILE *fp;
    fp=fopen(name,"r");
    if(fp==NULL){

```

```

        puts("open error");
    }
    for(i=0;;i++){
        *N=i;
        fscanf(fp,"%lf",&R[i]);
        fscanf(fp,"%lf",&V[i]);
        if(feof(fp)!=0) break;
    }
    fclose(fp);
}

void main(void)
{
    int i,n_pa12,n_pa23,n_h1,n_h2,n_h3,k;
    char ch,name_x1[15],name_y1[15],name_x2[15],name_y2[15],name_pa12[15],
    name_pa23[15],name_h1[15],name_h2[15],name_h3[15],name_b1[15],
    name_b2[15];
    double b,v,bf;
    double r=-9.0,t;
    double x1,x2,x3,y1,y2,y3;
    double r_pa12[150],pa12[150],r_pa23[150],pa23[150],r_h1[150],hh1[150],
    r_h2[150],hh2[150],r_h3[150],hh3[150];
    double d2_pa12[150],d2_pa23[150],d2_h1[150],d2_h2[150],d2_h3[150];
    FILE *fp_x1,*fp_y1,*fp_x2,*fp_y2,*fp_b1,*fp_b2;
    printf(" input value \n");
    input_v:
    printf("\n\t v (400-800 km/s) = ");
    scanf("%lf",&v);
    v=v/(2.1876e3);
    printf("\n\t b start at (bohr)= ");
    scanf("%lf",&b);
    printf("\n\t b final at (bohr)= ");
    scanf("%lf",&bf);
    printf("\n\t input filename P+A 12 to read : ");
    scanf("%s",name_pa12);
    printf("\n\t input filename P+A 23 to read : ");
    scanf("%s",name_pa23);
    printf("\n\t input filename h1 to read : ");
    scanf("%s",name_h1);
    printf("\n\t input filename h2 to read : ");
    scanf("%s",name_h2);
    printf("\n\t input filename h3 to read : ");
    scanf("%s",name_h3);
    printf("\n\t input filename to write x1 : ");
    scanf("%s",name_x1);
    fp_x1=fopen(name_x1,"w");
    if(fp_x1==NULL)
    {
        puts("open error");
    }
    printf("\n\t input filename to write y1 : ");
    scanf("%s",name_y1);
    fp_y1=fopen(name_y1,"w");
    if(fp_y1==NULL)
    {
        puts("open error");
    }
    printf("\n\t input filename to write x2 : ");
    scanf("%s",name_x2);
    fp_x2=fopen(name_x2,"w");
    if(fp_x2==NULL)
    {
        puts("open error");
    }
}

```



```

printf("\n\t input filename to write y2 : ");
scanf("%s",name_y2);
fp_y2=fopen(name_y2,"w");
if(fp_y2==NULL)
{
puts("open error");
}

printf("\n\t input filename to write P1(b) : ");
scanf("%s",name_b1);
fp_b1=fopen(name_b1,"w");
if(fp_b1==NULL){
puts("open error");
}

printf("\n\t input filename to write P2(b) : ");
scanf("%s",name_b2);
fp_b2=fopen(name_b2,"w");
if(fp_b2==NULL){
puts("open error");
}

read(r_pa12,pa12,&n_pa12,name_pa12);
read(r_pa23,pa23,&n_pa23,name_pa23);
read(r_h1,hh1,&n_h1,name_h1);
read(r_h2,hh2,&n_h2,name_h2);
read(r_h3,hh3,&n_h3,name_h3);
cubic_splines(r_pa12,pa12,d2_pa12,n_pa12);
cubic_splines(r_pa23,pa23,d2_pa23,n_pa23);
cubic_splines(r_h1,hh1,d2_h1,n_h1);
cubic_splines(r_h2,hh2,d2_h2,n_h2);
cubic_splines(r_h3,hh3,d2_h3,n_h3);
k=0;
do{
x1=1.0;x2=0.0;x3=0.0;y1=0.0;y2=0.0;y3=0.0;
t=-((sqrt(((r*r)-(b*b))/(v*v))));
Runge_kutta(r,b,v,t,&x1,&y1,&x2,&y2,&x3,&y3,r_pa12,pa12,d2_pa12,
r_pa23,pa23,d2_pa23,r_h1,hh1,d2_h1,r_h2,hh2,d2_h2,r_h3,
hh3,d2_h3,n_pa12,n_pa23,n_h1,n_h2,n_h3);
fprintf(fp_x1," %lf %lf\n",b,x2);
fprintf(fp_y1," %lf %lf\n",b,y2);
fprintf(fp_x2," %lf %lf\n",b,x3);
fprintf(fp_y2," %lf %lf\n",b,y3);
fprintf(fp_b1," %lf %lf\n",b,x2*x2+y2*y2);
fprintf(fp_b2," %lf %lf\n",b,x3*x3+y3*y3);
if((k%100)==0){
printf("\n\n%lf %lf %lf %lf %lf",b,
x1*x1+y1*y1,x2*x2+y2*y2,x3*x3+y3*y3,x1*x1+y1*y1+x2*x2+y2*y2+x3*x3+y3*y3);
k+=1;
}
b+=0.0005;
} while(b<=bf);
printf("Finish");
}

```

Appendix D

Program for Transforming an Adiabatic Potential to be Diabatic

A flow chart of this program is presented in Figure 3.2.

```
/* Transform to diabatic */
#include <stdio.h>
#include <math.h>
#include "nrutil.h"
#define dr .01
#define NOY .000001
#define PI 3.141592653589793
#define NS 5 /* number of electronic states */
main()
{
    double **c,**cc,**cin,**ch,**uu,**uua;
    double **u,r,rmin,rmax;
    int i,j,k,m,kmax;
    FILE *fp;
    void transmat();
    void inverse();
    void koon();
    void initpot();
    fp=fopen("diab.dat","w");
    if(fp==NULL){
        puts("open error");
    }
    printf("\n");
    printf("input initial distance : "); scanf("%lf",&rmin);
```



```

printf("input final distance : "); scanf("%lf",&rmax);
kmax=ceil((rmax-rmin)/dr)+1;
printf("rmin=%lf rmax=%lf k=%d",rmin,rmax,kmax);
c=f3tensor(1,NS,1,NS,0,2000); u=f3tensor(1,NS,1,NS,0,2000);
cc=dmatrix(1,NS,1,NS);
cin=dmatrix(1,NS,1,NS);
uu=dmatrix(1,NS,1,NS);
uua=dmatrix(1,NS,1,NS);
ch=dmatrix(1,NS,1,NS);
transmat(c,kmax,rmin);
initpot(u,kmax,rmin);
for(k=0;k<=kmax;k++){
    for(i=1;i<=NS;i++){
        for(j=1;j<=NS;j++){
            cc[i][j]=ch[i][j]*c[i][j][k];
            uu[i][j]=u[i][j][k];
        }
    }
}
trpose(ch,cin,NS);
koon(cin,uu,uua,NS);
koon(uua,cc,uu,NS);
for(i=1;i<=NS;i++){
    for(j=1;j<=NS;j++){
        u[i][j][k]=uu[i][j];
    }
}
for(k=0,i=0;k<=kmax;k++){
    if(k%10==0) i+=1;
    fprintf(fp,"%d %d\n",i,NS);
    for(i=1;i<=NS;i++){
        for(j=1;j<=NS;j++){
            for(m=0,r=rmin;m<=kmax;r+=dr,m++){
                if(r<1){
                    if(m%5==0) fprintf(fp,"%lf ",u[i][j][m]);
                } else if(r>=1 && r<4){
                    if(m%10==0) fprintf(fp,"%lf ",u[i][j][m]);
                } else if(r>=4 && r<10){
                    if(m%30==0) fprintf(fp,"%lf ",u[i][j][m]);
                } else {
                    if(m%100==0) fprintf(fp,"%lf ",u[i][j][m]);
                }
            }
        }
        fprintf(fp,"\n");
    }
}
for(r=rmin,k=0;k<=kmax;r+=dr,k++){
    if(r<1){
        if(k%5==0) fprintf(fp,"%lf ",r);
    } else if(r>=1 && r<4){
        if(k%10==0) fprintf(fp,"%lf ",r);
    } else if(r>=4 && r<10){
        if(k%30==0) fprintf(fp,"%lf ",r);
    } else {
        if(k%100==0) fprintf(fp,"%lf ",r);
    }
}
}
free_f3tensor(c,1,NS,1,NS,0,2000);
free_dmatrix(cc,1,NS,1,NS);
free_dmatrix(cin,1,NS,1,NS);
free_dmatrix(uu,1,NS,1,NS);
free_dmatrix(uua,1,NS,1,NS);
free_dmatrix(ch,1,NS,1,NS);
}
void transmat(double ***c,int kmax,double rmin)
{

```

```

int i,j,k,n,m,l,s;
double ***pa,***F,r;
void integ();
void initcoup();
pa=f3tensor(1,5,1,5,0,2000);
F=f3tensor(1,5,1,5,0,2000);
initcoup(pa,c,F,kmax,rmin);
s=1;
for(n=0;;n++){ /*this loop for iteration */
    integ(pa,F,kmax);
l=0;
    s= -1*s;
    for(i=1;i<=5;i++){
        for(j=1;j<=5;j++){
            for(k=0;k<=kmax;k++){
                c[i][j][k]+=s*F[i][j][k];
                if(fabs(F[i][j][k])>=NOY) l=1;
            }
        }
    }
    free_f3tensor(pa,1,NS,1,NS,0,2000);
    free_f3tensor(F,1,NS,1,NS,0,2000);
}
void read(double R[],double V[],int *N,char name[])
{
    int i;
    FILE *fp;
    fp=fopen(name,"r");
    if(fp==NULL){
        puts("open error");
    }
    for(i=0;;i++){
        *N=i;
        fscanf(fp,"%lf",&R[i]);
        fscanf(fp,"%lf",&V[i]);
        iffeof(fp)!=0 break;
    }
    fclose(fp);
}
void cubic_splines(double z[],double Bx[],double d2x[],int n)
{
    int i,j,k,N;
    double A[n+1][n+1],bx[n+1],koon,beta[n+1],rho[n+1];
    N = n-1;
    for(i=0;i<=N;i++){
        for(j=0;j<=N;j++){
            A[i][j] = 0.;
        }
    }
    for(i=1;i<=N-1;i++){
        A[i][i] = 2.0*(z[i+1]-z[i-1]);
        A[i][i+1] = z[i+1]-z[i];
        A[i][i-1] = z[i]-z[i-1];
        bx[i] = 6.0*((Bx[i+1]-Bx[i])/(z[i+1]-z[i])
            -(Bx[i]-Bx[i-1])/(z[i]-z[i-1]));
    }
    for(i=2;i<=N-1;i++){
        koon = -A[i][i-1]/A[i-1][i-1];
        A[i][i] += koon*A[i-1][i];
        bx[i] += koon*bx[i-1];
    }
    d2x[N-1]=bx[N-1]/A[N-1][N-1];
    for(i=N-2;i>=1;i--){

```

```

        d2x[i] = (bx[i]-A[i][i+1]*d2x[i+1])/A[i][i];
    }
    d2x[0] = 0.0;
    d2x[N] = 0.0;
}
double interpolate(double z,int n,double Z[],double B[],double d2[])
{
    int i,N;
    double D1,D2,DD,T1,T2,T3,T4,Mag;
    z=fabs(z);
    N=n-1;
    if( z<Z[0] || z>Z[N] ){
        printf("\nThere are not enough data");
        exit(1);
    }
    for(i=0;i<=N-1;i++){
        if((z > Z[i] && z < Z[i+1]) || z == Z[i] || z == Z[i+1]) {
            D1 = Z[i+1]-z;
            D2 = z-Z[i];
            DD = Z[i+1]-Z[i];
            T1 = ( d2[i]*D1*D1*D1 ) / ( 6.0*DD );
            T2 = ( d2[i+1]*D2*D2*D2 ) / ( 6.0*DD );
            T3 = ( (B[i+1]/DD) - (d2[i+1]*DD/6.0) ) * D2;
            T4 = ( (B[i]/DD) - (d2[i]*DD/6.0) ) * D1;
            Mag = T1+T2+T3+T4;
        }
    }
    return Mag;
}
void integ(double ***pa,double ***F,int kmax)
{
    int i,j,k,l,m;
    double **g;
    g=dmatrix(1,NS,1,NS);
    for(m=0;m<=kmax;m++){
        for(i=1;i<=5;i++){
            for(j=1;j<=5;j++){
                g[i][j]=0.;
                for(k=m+1;k<=kmax-1;k++){
                    for(l=1;l<=5;l++)
                        g[i][j]+=pa[i][l][k]*F[l][j][k]*dr;
                }
                for(l=1;l<=5;l++)
                    g[i][j]+=pa[i][l][m]*F[l][j][m]*dr/2.
                    +pa[i][l][kmax]*F[l][j][kmax]*dr/2.;
            }
        }
        for(i=1;i<=5;i++){
            for(j=1;j<=5;j++) F[i][j][m]=g[i][j];
        }
    }
    free_dmatrix(g,1,NS,1,NS);
}
void initpot(double ***u,int kmax,double rmin)
{
    int i,j,k,nh_s1,nh_s2,nh_s3,nh_p1,nh_p2;
    double rh_s1[200],h_s1[200],rh_s2[200],h_s2[200],rh_s3[200],h_s3[200],
        rh_p1[200],h_p1[200],rh_p2[200],h_p2[200];
    double d2h_s1[200],d2h_s2[200],d2h_s3[200],d2h_p1[200],d2h_p2[200],r;
    char name_hs1[15],name_hs2[15],name_hs3[15],name_hp1[15],name_hp2[15];
    double interpolate();
    void read();
    void cubic_splines();
    printf("\n\tinput filename of 1sigma potential : ");
}

```

```

scanf("%s",name_hs1);
printf("\n\t input filename of 2sigma potential : ");
scanf("%s",name_hs2);
printf("\n\t input filename of 3sigma potential : ");
scanf("%s",name_hs3);
printf("\n\t input filename of 1pi   potential : ");
scanf("%s",name_hp1);
printf("\n\t input filename of 2pi   potential : ");
scanf("%s",name_hp2);
read(rh_s1,h_s1,&nh_s1,name_hs1);
read(rh_s2,h_s2,&nh_s2,name_hs2);
read(rh_s3,h_s3,&nh_s3,name_hs3);
read(rh_p1,h_p1,&nh_p1,name_hp1);
read(rh_p2,h_p2,&nh_p2,name_hp2);
cubic_splines(rh_s1,h_s1,d2h_s1,nh_s1);
cubic_splines(rh_s2,h_s2,d2h_s2,nh_s2);
cubic_splines(rh_s3,h_s3,d2h_s3,nh_s3);
cubic_splines(rh_p1,h_p1,d2h_p1,nh_p1);
cubic_splines(rh_p2,h_p2,d2h_p2,nh_p2);
/* input coupling matrix */
for(i=1;i<=5;i++){
    for(j=1;j<=5;j++){
        for(k=0;k<=kmax;k++){
            u[i][j][k]=0.;
        }
    }
}
for(k=0,r=rmin;k<=kmax;k++,r+=dr){
    u[1][1][k]=interpolate(r,nh_s1,rh_s1,h_s1,d2h_s1);
    u[2][2][k]=interpolate(r,nh_s2,rh_s2,h_s2,d2h_s2);
    u[3][3][k]=interpolate(r,nh_s3,rh_s3,h_s3,d2h_s3);
    u[4][4][k]=interpolate(r,nh_p1,rh_p1,h_p1,d2h_p1);
    u[5][5][k]=interpolate(r,nh_p2,rh_p2,h_p2,d2h_p2);
}
}

void initcoup(double ***pa,double ***c,double ***F,int kmax,double rmin)
{
    int i,j,k,n_pa12,n_pa23,n_pa45;
    double r_pa12[200],pa12[200],r_pa23[200],pa23[200],r_pa45[200],pa45[200];
    double d2_pa12[200],d2_pa23[200],d2_pa45[200],r;
    char name_pa12[15],name_pa23[15],name_pa45[15];
    double interpolate();
    void read();
    void cubic_splines();
    printf("\n\t input filename of 1sigma-2sigma coupling : ");
    scanf("%s",name_pa12);
    printf("\n\t input filename of 2sigma-3sigma coupling : ");
    scanf("%s",name_pa23);
    printf("\n\t input filename of 1pi-2pi coupling : ");
    scanf("%s",name_pa45);
    read(r_pa12,pa12,&n_pa12,name_pa12);
    read(r_pa23,pa23,&n_pa23,name_pa23);
    read(r_pa45,pa45,&n_pa45,name_pa45);
    cubic_splines(r_pa12,pa12,d2_pa12,n_pa12);
    cubic_splines(r_pa23,pa23,d2_pa23,n_pa23);
    cubic_splines(r_pa45,pa45,d2_pa45,n_pa45);
    /* input coupling matrix */
    for(i=1;i<=5;i++){
        for(j=1;j<=5;j++){
            for(k=0;k<=kmax;k++){
                pa[i][j][k]=0.;
                if(i==j) { c[i][j][k]=F[i][j][k]=1.;}
            }
        }
    }
}

```

```

        else      { c[i][j][k]=F[i][j][k]=0.;}
    }
}
for(k=0,r=rmin;k<=kmax;k++,r+=dr){
    pa[1][2][k]=interpolate(r,n_pa12,r_pa12,pa12,d2_pa12);
    pa[2][3][k]=interpolate(r,n_pa23,r_pa23,pa23,d2_pa23);
    pa[4][5][k]=interpolate(r,n_pa45,r_pa45,pa45,d2_pa45);
/* coupling is symmetric hermitian */
pa[2][1][k]=-pa[1][2][k];
pa[3][2][k]=-pa[2][3][k];
pa[5][4][k]=-pa[4][5][k];
}
}

```



สถาบันวิทยบริการ
จุฬาลงกรณ์มหาวิทยาลัย

Curriculum Vitae



Saree Phongphanphanee

1974 Born on March, 15th in Bangkok, THAILAND.

1992-1996 Bachelor of Science (Physics),
Chulalongkorn University, Bangkok, THAILAND.

สถาบันวิทยบริการ
จุฬาลงกรณ์มหาวิทยาลัย